ADVANCED MATERIALS
www.advmat.de

Redox Targeting of Energy Materials for Energy Storage and Conversion

*Feifei Zhang, Mengqi Gao, Shiqiang Huang, Hang Zhang, Xun Wang, Lijun Liu, Ming Han, and Qing Wang**

The redox-targeting (RT) process or redox-mediated process, which provides great operation flexibility in circumventing the constraints intrinsically posed by the conventional electrochemical systems, is intriguing for various energy storage and conversion applications. Implementation of the RT reactions in redox-flow cells, which involves a close-loop electrochemical–chemical cycle between an electrolyte-borne redox mediator and an energy storage or conversion material, not only boosts the energy density of flow battery system, but also offers a versatile research platform applied to a wide variety of chemistries for different applications. Here, the recent progress of RT-based energy storage and conversion systems is summarized and great versatility of RT processes for various energy-related applications is demonstrated, particularly for large-scale energy storage, spatially decoupled water electrolysis, electrolytic N_2 reduction, thermal-to-electrical conversion, spent battery material recycling, and more. The working principle, materials aspects, and factors dictating the operation are highlighted to reveal the critical roles of RT reactions for each application. In addition, the challenges lying ahead for deployment are stated and recommendations for addressing these constraints are provided. It is anticipated that the RT concept of energy materials will provide important implications and eventually offer a credible solution for advanced large-scale energy storage and conversion.

1. Introduction

The ever-increasing energy demand and environmental concerns call for innovative energy technologies which effectively exploit various energy sources, particularly those of the sustainable solar and wind energy, and the ubiquitous waste heat.[1] However, despite their abundancy, the intermittency of these renewable energy sources and the distributed nature of waste heat necessitate advancements in both energy conversion and storage (in either electricity or chemical forms) adapting to the ways of harvesting them.[2] A wide variety of electrochemical systems have been employed to achieve energy conversion or storage. For instance, redox flow batteries (RFBs) with decoupled energy storage and power generation[3] are promising for grid electricity storage; electrolytic water splitting[4] especially using electricity from renewable energy sources is emerging as an important means for green hydrogen production; judiciously designed thermo-electrochemical processes are intriguing to constantly convert low-grade heat to electricity.[5]

Although the reaction mechanisms and active materials across different electrochemical energy storage and conversion systems vary broadly, they share some common issues prohibiting their widespread deployment. As an electrochemical system, the electrochemical reactions take place on the surface of electrode and at the electrode–electrolyte interface, which means that the storage or conversion capability of the cell would be inherently constrained by the surface area of electrode sheet and/or the volume of electrode compartment, in addition to other physical properties (electric, catalytic, geometric, etc.) of the electrode material.[6] Considering the active materials could be in gaseous, liquid or solid phase, judiciously designed electrode architecture is generally required to facilitate the reactions so that the materials are electrochemically accessible for a full utilization of their capacity. This is especially so when the reactants or products lack electric conductivity.[7] For instance, the round-trip energy efficiency of aprotic lithium–oxygen batteries is limited by the sluggish three-phase reactions of insoluble and insulating Li_2O_2 on the air cathode: oxygen reduction reaction (ORR) upon discharging and oxygen evolution reactions (OER) upon charging.[8] Similarly, water electrolysis requires rapid removal of gas bubbles from the surface of electrode in order to reduce the overpotentials of interfacial charge transfer and mass transport. In addition, while RFBs solve the storage issue by introducing separate electrolyte tanks so that an extended energy storage capability is accomplished, active materials dissolved in electrolyte solution generally present a low energy density due to their limited

F. Zhang, M. Gao, S. Huang, H. Zhang, X. Wang, Q. Wang
Department of Materials Science and Engineering
National University of Singapore
Singapore 117576, Singapore
E-mail: msewq@nus.edu.sg
L. Liu, M. Han
Clean Energy Research Centre
Temasek Polytechnic
Singapore 529757, Singapore
The ORCID identification number(s) for the author(s) of this article can be found under https://doi.org/10.1002/adma.202104562.

DOI: 10.1002/adma.202104562

solubility.[9] Hence, it is intuitively desired to develop innovative means to circumvent the constraints intrinsically imposed by the electrode in conventional electrochemical processes.

In 2006, Wang et al. reported an approach by employing redox mediators (RMs) dissolved in electrolyte to chemically address the poorly conducting battery materials through a so-called "redox targeting (RT)" process and increase the charge capacity and energy density.[10] During this process, the RMs first receive electrons or holes from the electrode via a conventional electrochemical process, and then chemically react with the battery material which is electrically segregated from the electrode. The RMs are then regenerated on the electrode through solution phase mass transport (diffusion or electrolyte flow) for the next round of reaction. With such a RT reaction, the solid battery materials are physically liberated from the current collector and could be placed in separate energy storage tanks, which led to the advent of RT-based flow battery (RTFB) in 2013. RTFB operates as a flow battery while the energy is mostly stored in solid materials as the conventional batteries. It thus breaks the boundary of the solid phase and liquid phase energy storage and provides an intriguing approach for large-scale energy storage.[11]

Herein, by reviewing the latest advancements, we attempt to demonstrate the great versatility and prospects of RT processes for energy-related applications, in particular, those for large-scale energy storage, thermal-to-electrical conversion, spatially decoupled water electrolysis, electrolytic N_2 reduction, as well as spent battery material recycling, and so on. The working principle, factors dictating the operation, exciting new progress, and future development associated with the respective application will be discussed and analysed to delineate the great potential of RT-based platform technology in addressing the pressing challenges of energy and sustainability.

2. RT Process – A Close-Loop Electrochemical–Chemical Cycle

The RT process or redox-mediated process is ubiquitous in various electrochemical systems and proceeds via a close-loop electrochemical–chemical cycle. As above stated, it generally involves a chemical reaction between an electrolyte-borne RM electrochemically generated on the electrode and a material (generally in solid form insoluble in electrolyte) off the electrode, which provides great flexibility in operation in circumventing the constraints intrinsically confronted by the conventional electrochemical systems. Depending on the nature of RT reactions, such a redox-mediated process when it is associated with the reaction of a RM with an energy storage or energy conversion material in tandem with the reversible electrochemical reaction of the RM on electrode, is intriguing for various energy storage and conversion applications.

Figure 1 illustrates the different RT processes for a wide variety of energy-related applications. As shown in Figure 1a, the electrochemical–chemical process of RMs shuttling and exerting charge exchanges between the electrodes and energy storage materials in the reactor tanks, enable decoupled charge storage in solid materials without contact with the electrode. Such an operation mode leads to RTFBs, which have the merits of operation flexibility, scalability, and safety as the RFBs, and meanwhile considerably enhanced energy density as the solid electrode batteries.[12] Upon operation, the soluble redox-active species in electrolytes are pumped and circulated between the electrode compartments and the external energy storage tanks as conventional RFBs. However, the RT reactions between the redox species and solid storage materials in the reactor tank extend the charge storage capability of the system from liquid phase to solid phase energy storage. The volumetric capacity is thus no longer limited by the concentration of electrolyte, but the solid active materials stored in tank, which in theory are on par with the solid electrode batteries. Moreover, different from the "semi-solid" flow cells which employ flowable viscous slurry containing solid electroactive materials and conductive additives to form a continuous charge percolating network in electrolyte, the electrolyte fluids in RTFBs remain the same as conventional RFBs, and in theory, no conductive additive is required for the solid energy storage materials.

The RT process based on an electrochemical–chemical cycle has gone well beyond energy storage. For instance, the RT reactions between RM and charge storage material of suitable temperature coefficient could considerably boost the thermo-electrical conversion efficiency when it operates over a thermally regenerative electrochemical cycle (TREC).[13] In addition, as depicted in Figure 1b, the electrochemically generated RM could initiate useful chemical reactions by transferring charges to reactants (in liquid or gaseous forms) on the surface of a heterogeneous catalyst loaded in the reactor tank. Such an electrochemical–chemical process could be used for catalytic water splitting, nitrogen reduction reaction (NRR), and CO_2 reduction reaction (CO_2RR).[14] In conventional electrolytic processes, the performance of electrolyzer is intimately dependent on the properties of electrocatalysts and mass transport toward the electrodes.[15] The electrocatalysts are employed to lower the energy barrier of the electrochemical reactions and promote the charge transfer kinetics on their surface,[16] which thus should have large surface area with active sites for fast interfacial charge transfer, and meanwhile in good electrical contact with the electrode and reduced path length for rapid ion and electron transport.[17] In contrast, the RT process provides an alternative approach which liberates the catalyst from the electrode surface and alleviates the critical requirements for electrocatalyst in terms of mass/charge transport and thus the conductivity. The RM carries electrons from electrode to localized catalyst bed and facilitates the catalytic reaction in the tank. With semiconducting photoanode or photocathode which absorbs light to generate energetic electrons or holes, a spatially decoupled photosynthetic process could be realized.[14c]

3. RT-Based Energy Storage

3.1. RT-Based Flow Batteries (RTFB)

For any RT processes, the potential difference between the redox molecule and material provides the driving force for interfacial charge transfer. In order to promote the RT reactions, in the early development of RTFB, one solid energy storage material was usually paired with two redox mediators

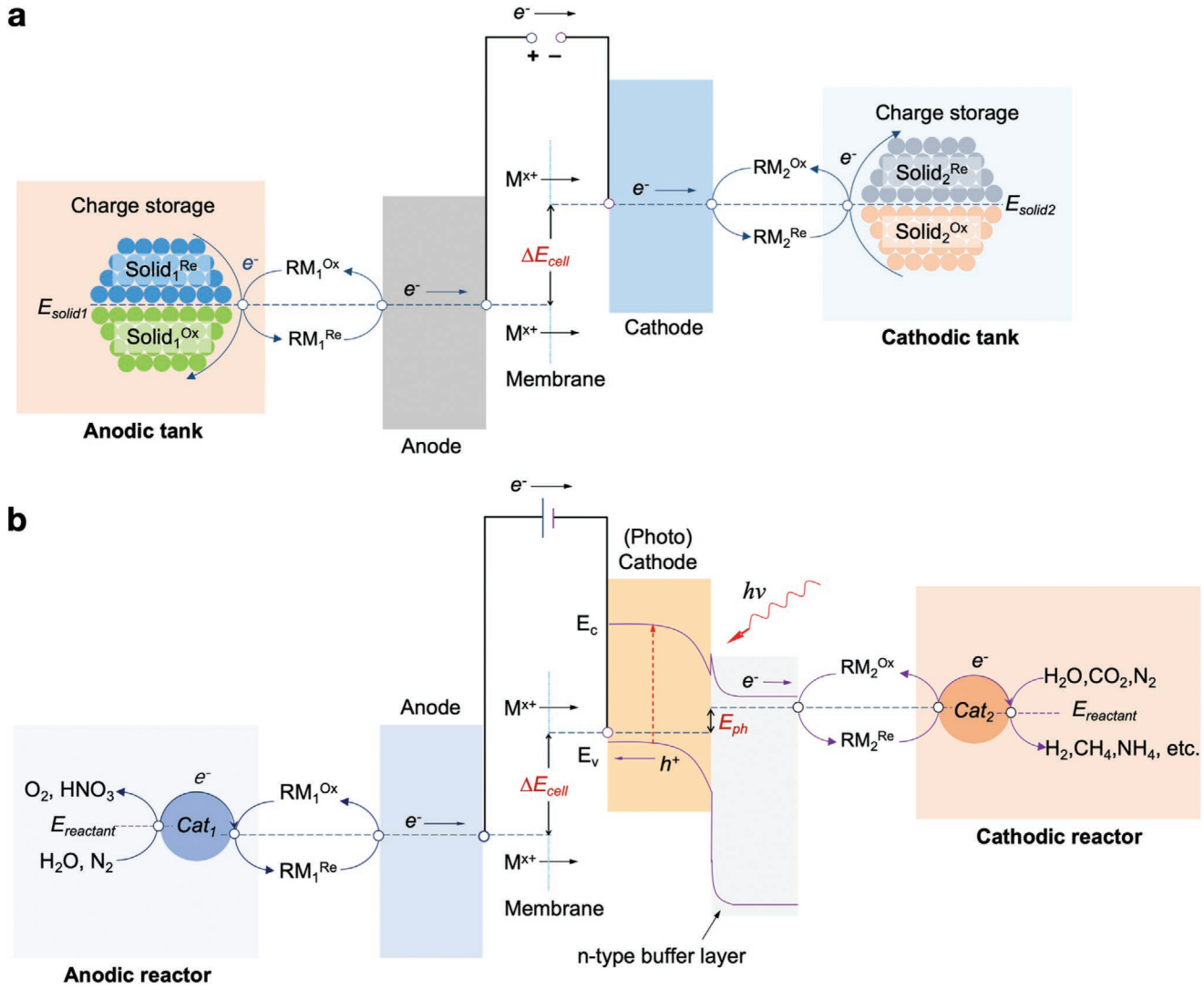

Figure 1. A panoramic energy diagram showing the working principles of two typical RT-based electrochemical systems for a) electrochemical energy storage with two energy storage tanks and b) (photo) electrochemical conversion with two reactor tanks. ΔE_{cell} is the voltage applied during an electrolytic process or electromotive force generated during a galvanic process. E_{ph} is the photovoltage generated by the photocathode. As an example, the two electrode compartments here are separated by cation-exchange membrane.

with potentials straddling that of the solid material to achieve two-way RT reactions during the charge and discharge processes. As shown in **Figure 2**a, the one with higher potential oxidizes the solid material during charging and the one with lower potential reduces the solid material during discharge. As a result, the energy storage materials could be reversibly charged and discharged via the RT reactions with the two RMs. This allows greater flexibility for the selection of suitable RMs for facilitated RT reactions.

3.1.1. Non-Aqueous RTFB

Compared with other battery chemistries, lithium-ion batteries (LIBs) enjoy great advantage in energy density largely because of the high effective concentration of charges stored in the electrode materials (in addition to large cell voltage), for instance, 22.8 M in $LiFePO_4$, and more.[19] To leverage both the operation flexibility of RFBs and high energy density of LIBs, redox flow lithium-ion battery (RFLB) was devised resorting to the interplay of the electroactive materials between non-aqueous redox active electrolytes of RFBs and solid active materials of LIBs, via RT reactions. In an RFLB, the solid electrode materials are loaded in the cathodic and anodic tanks. Upon operation, these materials remain static, while the stored charges are delivered to the electrodes by the flow of dissolved RMs through reversible chemical lithiation/delithiation reactions with the materials.[20]

In 2013, Huang et al. reported the first RFLB half-cell which used $LiFePO_4$ (3.45 V vs Li/Li^+) as the Li^+– storage material in the cathodic tank, while ferrocene (Fc, 3.25 V vs Li/Li^+) and 1,1′-dibromoferrocene ($FcBr_2$, 3.55 V vs Li/Li^+) were selected as the redox mediators in the catholyte.[11] The anodic half-cell was reported in 2014 by Pan et al., in which TiO_2 (1.80 V vs Li/Li^+)

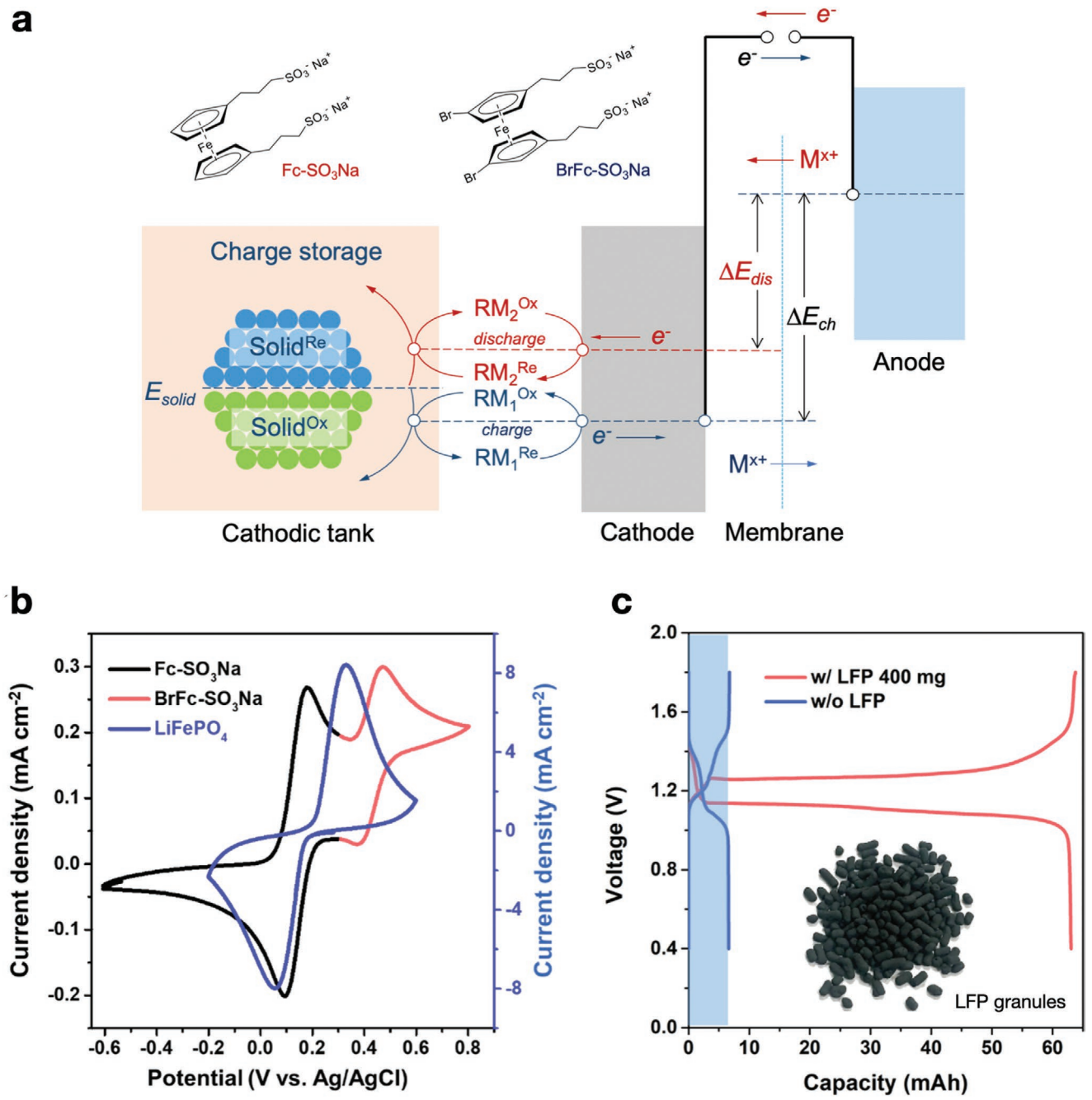

Figure 2. a) Energy diagram showing the working principles of a RTFB cathodic half-cell by using two redox mediators with potentials straddling that of the cathodic solid charge storage material. b) Cyclic voltammograms (CV) of $LiFePO_4$ and two ferrocene derivatives Fc–SO_3Na and BrFc–SO_3Na. The potential of $LiFePO_4$ is between that of the two mediators. Reproduced with permission.[18] Copyright 2020, Elsevier. c) Voltage profiles of a Zn–Fc–SO_3Na/BrFc–SO_3Na flow battery with and without $LiFePO_4$ granules loaded in the cathodic tank. The inset shows the photograph of $LiFePO_4$ granules. Adapted with permission.[18] Copyright 2020, Elsevier.

was used as the Li-storage material, while cobaltocene ($CoCp_2$, 1.90 V vs Li/Li^+) and bis(pentamethyl cyclopentadienyl) cobalt ($CoCp^*_2$, 1.36 V vs Li/Li^+) were selected as the RMs.[21] In 2015, an RFLB full cell was demonstrated using the above active materials and RMs.[22] During discharge process, electric power is generated via the electrochemical reactions of the RMs on the electrodes with charges constantly dispensed by solid materials in the tank. Among several other advantages, the energy density of RFLB can reach up to 500 Wh L^{-1}, 10 times as high as that of the vanadium flow battery (VFB).[23]

In 2019, Self et al. demonstrated a RTFB sodium battery half-cell.[24] Reversible sodium storage in red phosphorus loaded in an external packed-bed reactor was achieved with mediated reactions by a pair of soluble anion radical species biphenyl and pyrene in the absence of binders or conductive additives. This effectively unleashes the capacity of battery from the solubility

limit of redox species in the electrolyte and can conceivably achieve energy densities exceeding 200 Wh kg^{-1}. Very recently, an all organic RTFB was reported by Wong et al.[25] After tuning the steric and electronic properties of a series of organic RMs and viologen-based redox polymer material, the battery showed a high material utilization (>90%) and voltage efficiencies (>75%) in a preliminary study. While intriguing, the poor ionic conductivity of the membrane and non-aqueous electrolytes used in the above studies severely limit the power performance of the devices. Hence for near-term deployment, aqueous systems present a more pragmatic and implementable solution.

3.1.2. Aqueous RTFB

Conventional aqueous RFBs (e.g., VFB, Fe–Cr, Ce-based, etc.) generally employ transition metal ions in acidic solutions, which however confront challenges, such as high materials cost, crossover, and corrosive or hazardous electrolytes, preventing them from large-scale deployment.[3a] Recently, earth abundant redox-active organic molecules have received considerable attention as viable alternatives to the inorganic counterparts in RFBs.[26] However, these systems continue to suffer from low volumetric capacity as a result of the low solubility of RMs. As those revealed in the non-aqueous systems, the implementation of RT concept in these aqueous systems can considerably enhance the effective concentration of redox species and thus the capacity. In 2020, Yu et al. reported a pH-neutral aqueous flow battery system employing ferrocene derivatives as robust RMs.[18] The anionic Fc–SO_3Na manifested high caliber as a cathodic redox species which allows the use of cation-exchange membranes. When paired with Zn anode, the battery exhibited a prominent capacity retention of 99.9975% per cycle under 40 mA cm^{-2} after 1000 cycles. To enhance the energy density, $LiFePO_4$ (0.21 V vs Ag/AgCl) granules were loaded into the catholyte tank, while a pair of Fc-derivatives, BrFc–SO_3Na (0.41 V vs Ag/AgCl) and Fc–SO_3Na (0.13 V vs Ag/AgCl) with potentials straddling that of $LiFePO_4$ were used as redox mediators (Figure 2b). As shown in Figure 2c, with such a RT system, the catholyte volumetric capacity was boosted up to 293.5 Ah L^{-1}, representing a state-of-the-art two-molecule RTFB system.

3.2. Evolution of RTFBs

In the early demonstration of RT concept, two different RMs of suitable potentials were generally employed to pair with one active solid material in order to achieve two-way RT reactions.[27] The two-molecule RT system, however, generally induces voltage loss owing to their relatively large potential difference. For instance, the Fc and $FcBr_2$ bring about 300 mV voltage loss when paired with $LiFePO_4$, leading to a relatively low voltage efficiency.[11,28] Moreover, in a full cell demonstration, the two-molecule system comprises four different RMs and four stages of reactions, which brings great complexity to the operation compromising cycling stability of the cell.[19,29] To address these issues, single RMs with two redox reactions at potentials straddling that of the solid material have been investigated to accomplish reversible RT reactions of the latter. For instance, iodide species (I^-/I_3^- and I_3^-/I_2) and 2,3,5,6-tetramethylp-phenylenediamine have been separately reported to chemically lithiate/delithiate $LiFePO_4$.[30]

With the above attempts and development, single-molecule RT (SMRT) reaction was proposed in 2017, which operates upon "one molecule, one reaction" for one solid material and thus greatly simplifies the RT system.[31] In the SMRT reaction, the RM is required to have an identical redox potential to that of the targeted solid active material, and the reaction between the material and RM is only driven by the Nernstian potential difference induced by the activity changes of the redox species during charging and discharging. Therefore, the voltage profile of an SMRT battery exhibits only one charge/discharge plateau, which significantly eliminates the voltage hysteresis and enhances the round-trip energy efficiency.

3.2.1. Non-Aqueous SMRT-Based Flow Batteries

Zhou et al. reported a $LiFePO_4$-based RFLB cathodic half-cell enabled with the SMRT reactions in 2017.[31b] A ferrocene derivative ionic liquid (FcIL, 3.43 V vs Li/Li^+) with nearly identical redox potential to that of $LiFePO_4$ was judiciously designed. The diving force from the potential difference between the molecule and material is:

$$\Delta E = \frac{RT}{F} \ln \frac{a_{RM^+}}{a_{RM} \cdot a_{Li^+}} \tag{1}$$

During the charge process, more RM^+ is generated in the catholyte with the oxidation of RM on the electrode, and Li^+ ions migrate to the anodic compartment for charge balancing, which altogether lead to a positive ΔE. Conversely, more RM and Li^+ ions are accumulated in the catholyte, resulting in a negative ΔE during discharge process. The evolution of redox species at different states of charge/discharge (SOC/SOD) was monitored by operando UV–vis spectroscopy, which unambiguously validates the reversible SMRT reaction between FcIL and $LiFePO_4$. With the SMRT system, the free-energy loss which could have been induced by the multiple redox reactions is eliminated at large. As a result, the SMRT-based flow cell with a lean electrolyte composition has achieved unprecedentedly high voltage efficiency at an energy density of 330 Wh L^{-1}.

A variety of SMRT systems based on different battery chemistries have been reported. For instance, Zhou et al. demonstrated a SMRT-based redox flow sodium-ion battery using $Na_3V_2(PO_4)_3$ (NVP) as the sole energy storage material (**Figure 3**a).[32] With the multivalent property of vanadium, NVP could be used as both the cathode (3.40 V vs Na/Na^+) and anode (1.63 V vs Na/Na^+). To pair with NVP for both cathodic and anodic SMRT reactions, 10-methylphenothiazine (MPTZ) and 9-fluorenone (FL) which have identical redox potentials to the solid material were chosen as catholyte and anolyte RMs, respectively (Figure 3b). The kinetics of SMRT reaction between MPTZ and NVP was carefully studied with various steady-state techniques and was well described with the Butler–Volmer formulation at low overpotentials (Figure 3c). The SMRT reaction between the reduced FL and NVP in the anodic side was monitored with a fluorescence microscope (Figure 3d), from which

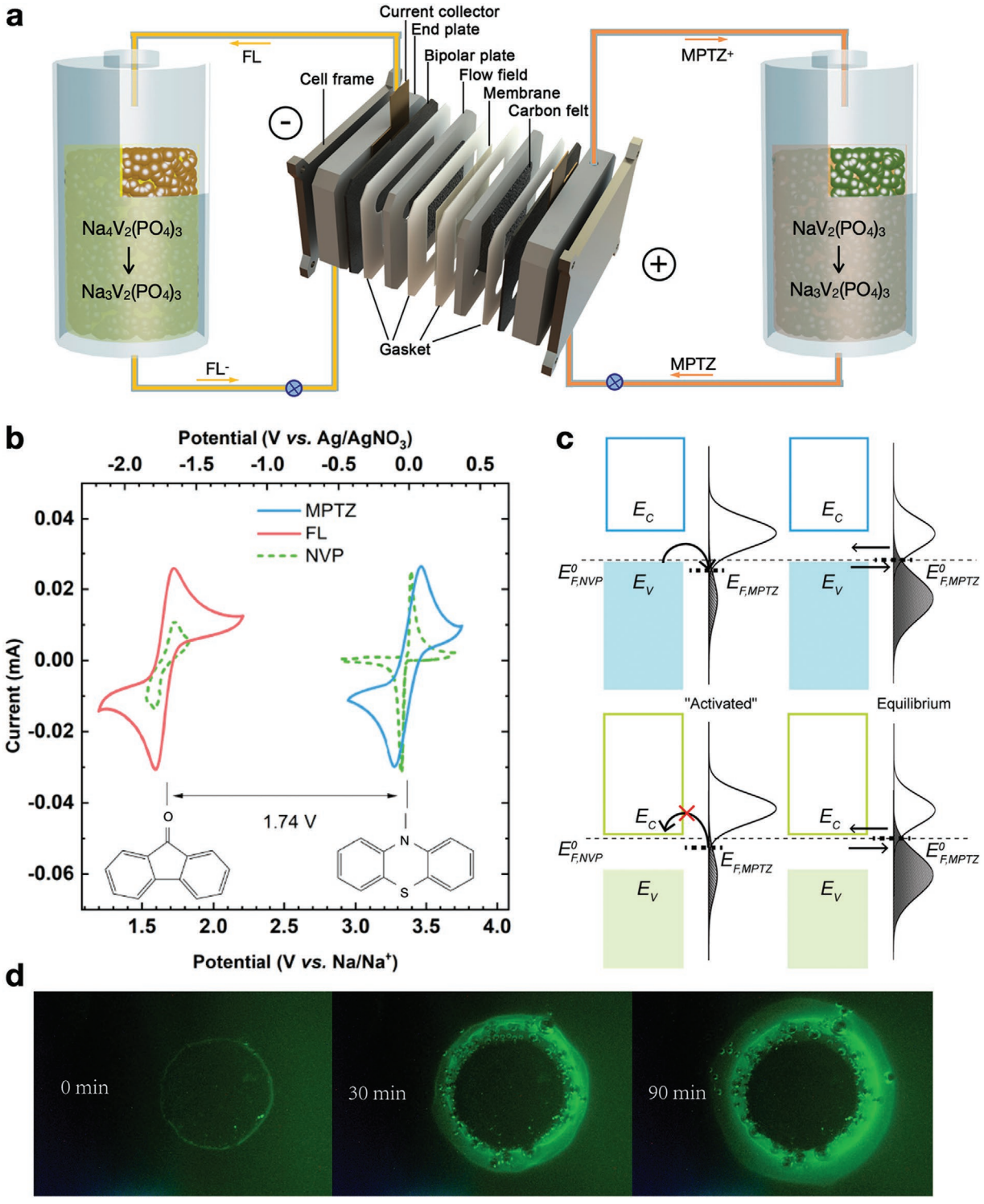

Figure 3. a) Schematic illustration of a SMRT-based redox flow sodium-ion battery during discharge process. It uses MPTZ and FL as the RM in catholyte and anolyte respectively, NVP as both the anodic and cathodic storage materials. Adapted with permission.[33] Copyright 2020, Wiley-VCH. b) CV curves of MPTZ in propylene carbonate and FL in G4/DMSO mixture, and those of $Na_3V_2(PO_4)_3$. c) Energy diagrams at different state of charge (SOC) of NVP and redox electrolyte. The upper and lower diagrams represent the energetics of the SMRT system with respect to $Na_3V_2(PO_4)_3$ and $NaV_2(PO_4)_3$, respectively. The diagrams on the left and right represent the conditions of "activated" and equilibrium SMRT reactions, respectively. d) Fluorescence microscopic images of a planar quartz reactor filled with 20 mM fully reduced FL upon reacting with a compact NVP granule assembly. The images were taken after 0, 30, and 90 min of reactions.[32] (b,d) Adapted with permission.[32] Copyright 2019, Wiley-VCH. (c) Reproduced with permission.[32] Copyright 2019, Wiley-VCH.

fluorescent FL (oxidized) emerged and propagated around the NVP granule with time was observed, suggesting a continuous reaction between the two. The anodic and cathodic capacity of such a SMRT-based redox flow sodium-ion battery full cell are 17 and 3 times higher than the solubility limit of respective electrolyte, and the energy density reached up to 88 Wh L^{-1}.

A variant of the SMRT reaction is the "self-mediated" reactions proposed by Lu and co-workers, between soluble polychalcogenides and insoluble ones for redox flow Li-chalcogen batteries.[34] The full self-mediated reactions are completed via a combination of electrochemical, comproportionation and disproportionation reactions of the inherently present polychalcogenides in the system at different stages of charge/discharge. Such a self-mediated flow battery demonstrated very high catholyte volumetric capacities of 1268 and 1096 Ah L^{-1} for Li–S and Li–Se, respectively. For practical operation, controllable formation of the insoluble species preferably in the tank during the charge process would be critical.

3.2.2. Aqueous SMRT-Based Flow Batteries

Despite the larger electrochemical window of organic electrolytes, the poor ionic conductivity and flammability of organic solvent and a lack of suitable ion-conducting membranes impede the development of non-aqueous RFLB. In 2018, Yu et al. reported an aqueous RFLB full cell based on the concept of SMRT reaction, for which $[Fe(CN)_6]^{4-/3-}$ and S^{2-}/S_2^{2-} were employed as the RMs in catholyte and anolyte, paired with $LiFePO_4$ and $LiTi_2(PO_4)_3$ as the cathodic and anodic energy storage materials, respectively.[35] The redox potential of S^{2-}/S_2^{2-} is –0.69 V versus Hg/HgO, consistent with that of $LiTi_2(PO_4)_3$, while the potential of $[Fe(CN)_6]^{4-/3-}$ is 100 mV more positive than $LiFePO_4$. TEGDME was then introduced as a cosolvent in the catholyte to adjust the potential of $[Fe(CN)_6]^{4-/3-}$ so that it exactly matches that of $LiFePO_4$. Such an aqueous RFLB has superior ionic conductivity in electrolyte and membrane, and faster reaction kinetics compared with its non-aqueous counterpart. As such, its power performance is considerably enhanced. A volumetric capacity of 76 and 141 Ah L^{-1} has been achieved for cathodic and anodic tank, respectively, which could potentially be further improved to 305 and 207 Ah L^{-1} by optimizing the utilization and loading of solid materials.

In 2019, Chen et al. introduced Prussian blue ($Fe_4[Fe(CN)_6]_3$, PB) as a robust and low-cost capacity boosting material in neutral aqueous RFBs.[36] The PB material presents two reversible redox reactions at 0.25 and 0.92 V (vs Ag/AgCl) in pH neutral solutions, which nearly coincides with that of $[Fe(CN)_6]^{4-/3-}$ and Br^-/Br_2, respectively (**Figure 4**a). The authors built a $[Fe(CN)_6]^{3-}$–Br^- flow cell with PB as the sole energy storage material in both the cathodic and anodic tanks, and the $[Fe(CN)_6]^{4-/3-}$/PB pair has presented a volumetric capacity of 61.6 Ah L^{-1}, corresponding to a 2.3 M of effective concentration of the electrolyte, which is two times above the solubility limit of $[Fe(CN)_6]^{4-/3-}$. Meanwhile, more than 50% utilization of PB was achieved at 20 mA cm^{-2}, with a capacity retention of >99.991% per cycle upon continuous tests (Figure 4b). When paired with a zinc anode, an impressive energy density of 97.4 Wh L^{-1} and an energy efficiency of 87.5% have been attained with a Zn–$[Fe(CN)_6]^{3-}$/PB flow cell at 20 mA cm^{-2} (Figure 4c). According to the neutron diffraction, density functional theory (DFT) calculations and operando spectroscopic measurements, the structural evolutions of PB were scrutinized upon reacting with $[Fe(CN)_6]^{4-/3-}$. Based on the robust SMRT system, a 500 W battery stack operating on PB/$Fe[(CN)_6]^{3-}$-S_x^{2-} chemistry has been fabricated, in which PB materials were assembled into different structures (honeycomb and mesh) by extrusion and 3D printing methods to facilitate the SMRT reactions while the electrolyte flows through the material in the tank (Figure 4d).

Following the success of PB-based SMRT reaction, a Prussian blue analogue (PBA) material $(VO)_6[Fe(CN)_6]_3$ was reported as the catholyte capacity booster for VFB by Cheng et al.[37] Leveraging the SMRT reaction with VO^{2+}/VO_2^+, such a vanadium-based PBA material (0.88 V vs Ag/AgCl) enabled a considerable enhancement in catholyte capacity. The theoretical volumetric capacity of the PBA material could reach 135 Ah L^{-1}, which is more than three times that of the conventional VFBs. More importantly, considering the catholyte of VFBs at higher concentrations suffers from inferior stability at elevated temperatures, by virtue of the SMRT reaction with PBA, the concentration of VO^{2+}/VO_2^+ in catholyte can be reduced to around 0.6 M without sacrificing the capacity. As a result, the operating temperature of the catholyte can be broadened from <40 °C to over 70 °C, providing a credible means for robust and high-density energy storage applications of VFBs without cooling.

In recent years, aqueous organic redox flow batteries (AORFBs) have attracted considerable attention due to the advantages of using earth-abundant materials, synthetic flexibility, and fast reaction kinetics, but the low solubility of the active materials remains a hurdle for high energy density. Zhou et al. reported a polyimide (PI, –0.27 V and –0.21 V vs SHE) material as the capacity booster for 9,10-anthraquinone-2,7-disulphonic acid (2,7-AQDS, –0.25 V vs SHE) in pH neutral conditions.[33] The capacity of 2,7-AQDS anolyte reached 97 Ah L^{-1} at 30 mA cm^{-2} with a solid material utilization as high as 83%. Combined with NaI-based catholyte and nickel hexacyanoferrate as the catholyte capacity booster, a full cell energy density of 39 Wh L^{-1} has been achieved via SMRT reactions on both sides.

In addition to the above advancements, Girault and co-workers reported a Fe–V aqueous flow cell using polyaniline as the capacity booster for both catholyte and anolyte in 2017.[31a] By mediating the emeraldine–pernigraniline transition of polyaniline, a threefold improvement in volumetric capacity was achieved for $Fe^{2+/3+}$ catholyte compared with the electrolyte alone. The same group also demonstrated the utilization of copper hexacyanoferrate to promote the capacity of *N,N,N*-2,2,6,6-heptamethylpiperidinyl oxy-4-ammonium chloride electrolyte, with which a high energy density of 97.2 Ah L^{-1} was achieved.[38] For alkaline flow batteries, $[Fe(CN)_6]^{4-/3-}$ has been one of the few choices for catholyte, but the energy density is limited by its low solubility. In 2019, Ventosa and co-workers reported a RT-based alkaline electrolyte system using $Ni(OH)_2$ as solid charge storage material to enhance the capacity of $[Fe(CN)_6]^{4-/3-}$, with which a volumetric capacity of 29 Ah L^{-1} was obtained.[39] When paired with phenazine, an energy density of 16 Wh L^{-1} was achieved based on total electrolyte volume.

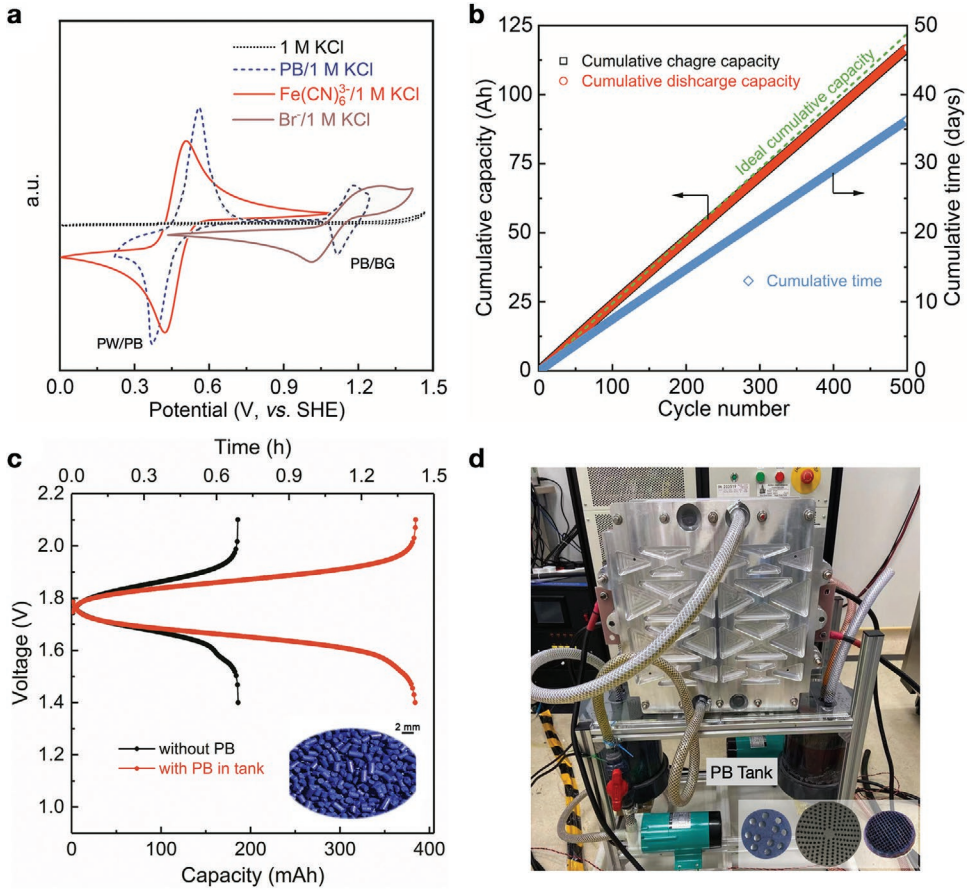

Figure 4. a) CV curves of Prussian blue (PB), $[Fe(CN)_6]^{4-/3-}$ and Br^-/Br_2 in 1 M KCl supporting electrolyte. Redrawn from ref. [36]. Copyright 2019, Elsevier. b) Cumulative capacity and time of the PB/$[Fe(CN)_6]^{4-/3-}$ symmetric cell undergoing 500 cycles of continuous testing at a current density of 20 mA cm^{-2}. Reproduced with permission.[36] Copyright 2019, Elsevier. c) Voltage profiles of a Zn–$[Fe(CN)_6]^{3-}$ full cell before and after adding PB granules in the cathodic tank. The inset shows a photograph of PB granules. Adapted with permission.[36] Copyright 2019, Elsevier. d) Photograph of a 500 W PB/$[Fe(CN)_6]^{3-}$–S_x^{2-} full cell stack with PB loaded in cathodic tank. The inset shows the photographs of honeycomb and mesh structured PB material made by extrusion (left and middle) and 3D printing (right), respectively.

3.3. RT-Based Redox Flow Li–O_2 Battery

Rechargeable Li–O_2 battery has considerably higher energy density than other battery chemistries.[40] When aprotic electrolyte is used, oxygen is reduced on the cathode forming Li_2O_2 during the discharge process, while it is electrochemically decomposed evolving oxygen upon charging.[41] However, the formation of insoluble and insulating Li_2O_2 on the surface of cathode during discharge process, leads to passivation and pore clogging of the air electrode,[42] which consequently gives rise to large voltage hysteresis, low power performance, and even premature termination of discharge.[43] During the charge process, the decomposition of Li_2O_2 requires large driving force, resulting in low round-trip energy efficiency.[44] Leveraging the electrochemical–chemical cycle, the electrochemical reactions of O_2/Li_2O_2 in conventional Li–O_2 battery could likewise proceed with redox-mediated chemical reactions off the electrode as those demonstrated in other RT processes. As a result, the above issues associated with surface passivation and pore clogging of the air electrode can be circumvented, and the primary advantages of Li–O_2 battery can thus be better harnessed.

The first RT-based redox flow Li–O_2 battery (RFLOB) was reported by Zhu et al. in 2015.[45] As the standard redox potential of O_2/Li_2O_2 couple is 2.96 V (vs Li/Li^+), iodine species (3.10/3.70 V vs Li/Li^+ for $I^-/I_3^-/I_2$) was used as RM for OER while ethyl viologen (EV, 2.65 V vs Li/Li^+) for ORR. In such a battery system, the three-phase electrochemical reaction on air electrode is reduced to one two-phase electrochemical reaction of RMs on electrode and one two-phase chemical reaction of RMs with oxygen species in a GDT, with which the formation and decomposition of Li_2O_2 are shifted from the electrode surface to GDT and proceed chemically without directly interfering the former. Thus, the energy efficiency and capacity are promoted. This is in addition to the enhanced operation flexibility by incorporating the decoupled flow battery design.

Later in 2016, another pair of RMs were selected for rechargeable RFLOB.[8b] Tris-{4-[2-(2-methoxyethoxy)ethoxy]-phenyl}-amine (TMPPA, 3.63 V vs Li/Li^+) was used to catalyze the OER process while 2,5-di-tert-butyl-1,4-benzoquinone (DTBBQ, 2.63 V vs Li/Li^+) was used for the ORR process. More recently, a complementary dual RMs system was employed to boost the power of RFLOB,[46] in which duroquinone (DQ) was introduced

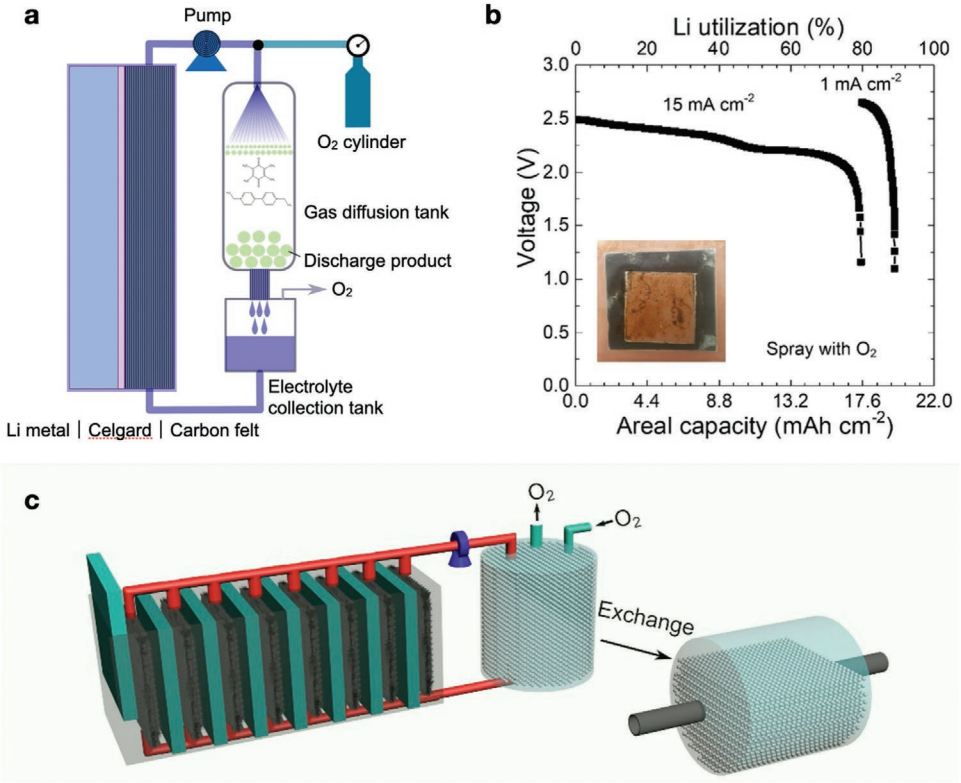

Figure 5. a) Configuration of a RFLOB (single cell) with integrated electrolyte spray. Adapted with permission.[46] Copyright 2018, The Royal Society of Chemistry. b) Discharge voltage profiles of RFLOB operated with electrolyte spray. The cells were fed with oxygen. The electrolyte was EV–DQ (0.2 M/0.2 M) in 1 M LiTFSI/DMSO. c) Illustration of the operation of an RFLOB cell system (stack) with exchangeable gas diffusion tank (GDT). The discharge products collected from GDT are recycled by capturing CO_2 to form a value-added product Li_2CO_3. (b,c) Reproduced with permission.[46] Copyright 2018, The Royal Society of Chemistry.

as a RM to catalyze the ORR process while EV was used as the other RM to eliminate the formation of soluble superoxide so that the formed Li_2O_2 is restricted inside the GDT where O_2 is fed in. As illustrated in **Figure 5**a, a spraying nozzle was integrated at the inlet of GDT to produce fine mists of electrolyte solution which are surrounded by O_2 atmosphere to further enhance the ORR reaction. With the EV–DQ (0.2 M/0.2 M) electrolyte spray and O_2 stream, the cell could steadily discharge at 15 mA cm^{-2} with nearly unity utilization of lithium metal (Figure 5b). An areal power of 60 and 34 mW cm^{-2} has been achieved when fed with O_2 and dry air, respectively. To recharge this RFLOB and examine the robustness of the redox-mediated ORR process, the authors demonstrated a method by mechanically refuelling Li metal to realize continuous operation. As illustrated in Figure 5c, the fuel can be fed into the cell by simply replenishing fresh Li foils in the anode compartment upon depletion. Because the discharge products accumulate in the GDT, the rest of the cell components, including the cathode and electrolyte, can operate uninterruptedly until the GDT tank is full which can then be replaced with an empty one.

In RTFBs, the utilization of solid material may become constrained by the sluggish kinetics of RT reactions, especially at high current densities. It is thus vital to search for highly dynamic RMs and charge storage material pairs that have rapid charge transfer kinetics. The two-molecule RT systems, while they have larger room for adjusting the driving force for interfacial charge transfer, have compromised voltage efficiency. In SMRT systems, due to the slanting voltage profiles of some electrode materials and the resulted mismatch of redox potentials, only a fraction of the capacity could be utilized by SMRT reaction, which results in reduced capacity. Moreover, the stability of RMs is also critical for the RTFBs, for which the RMs and solid active materials should undergo repeated reaction cycles during operation. This is especially so, considering the RMs act as mediators shuttling between the electrode and solid materials, during which one cycle of device operation entails multiple turnovers of RMs. To explore more efficient SMRT reactions, efforts are to be taken to screen robust redox species with tunable redox potentials by molecular engineering, so that matched potentials with those of energy storage materials and enhanced reaction kinetics could be achieved.

4. RT-Based Energy Conversion

RFBs have been extensively developed as a promising electrochemical energy storage technology for grid peak shaving and frequency regulation, and buffering the impact of intermittent electricity generated by solar and wind to the electrical grid. Based on a close-loop electrochemical–chemical process, RTFBs have shown combined benefits of both RFBs and solid electrode batteries to effectively store electricity in large scale. Going

beyond energy storage, the versatile RT reactions in tandem with the electrochemical reactions in the cell also provide intriguing approach for various energy conversion applications[13,47] and on-demand chemical synthesis.[14a,b,48] In particular, when the reactions are driven by the electricity generated from renewable while intermittent energy sources, the electrolytic flow cell design integrated with separate reactor tanks for various RT reactions endows the energy conversion process great operation flexibility and stability for practical applications.

4.1. RT-Based Thermal-To-Electrical Energy Conversion and Storage

A vast amount of low-grade heat (<100 °C) is generated in vehicles, electronics, industries, solar/geothermal energy, and biological entities, which is usually wasted due to the lack of effective recovery technologies.[5b,49] Integrating TREC to battery technology is an effective method for simultaneous thermal-to-electrical conversion and energy storage.[5c,50] However, for static TREC systems with solid materials as active species, their electrolytes with high heat capacity do not directly contribute to the thermoelectric conversion and energy storage, which greatly compromises the overall thermoelectric performance.[5a,51] On the contrary, for redox flow TREC systems with active materials dissolved in liquid electrolyte, the low charge density and high heat capacity limit their thermoelectric efficiency, which constrains their practical use for waste heat harnessing.[52]

The above problems could be elegantly solved by integrating the RT concept into TREC system.[13] As shown in **Figure 6**a, different from the traditional static or flow system with a single active material performing a single electrochemical reaction

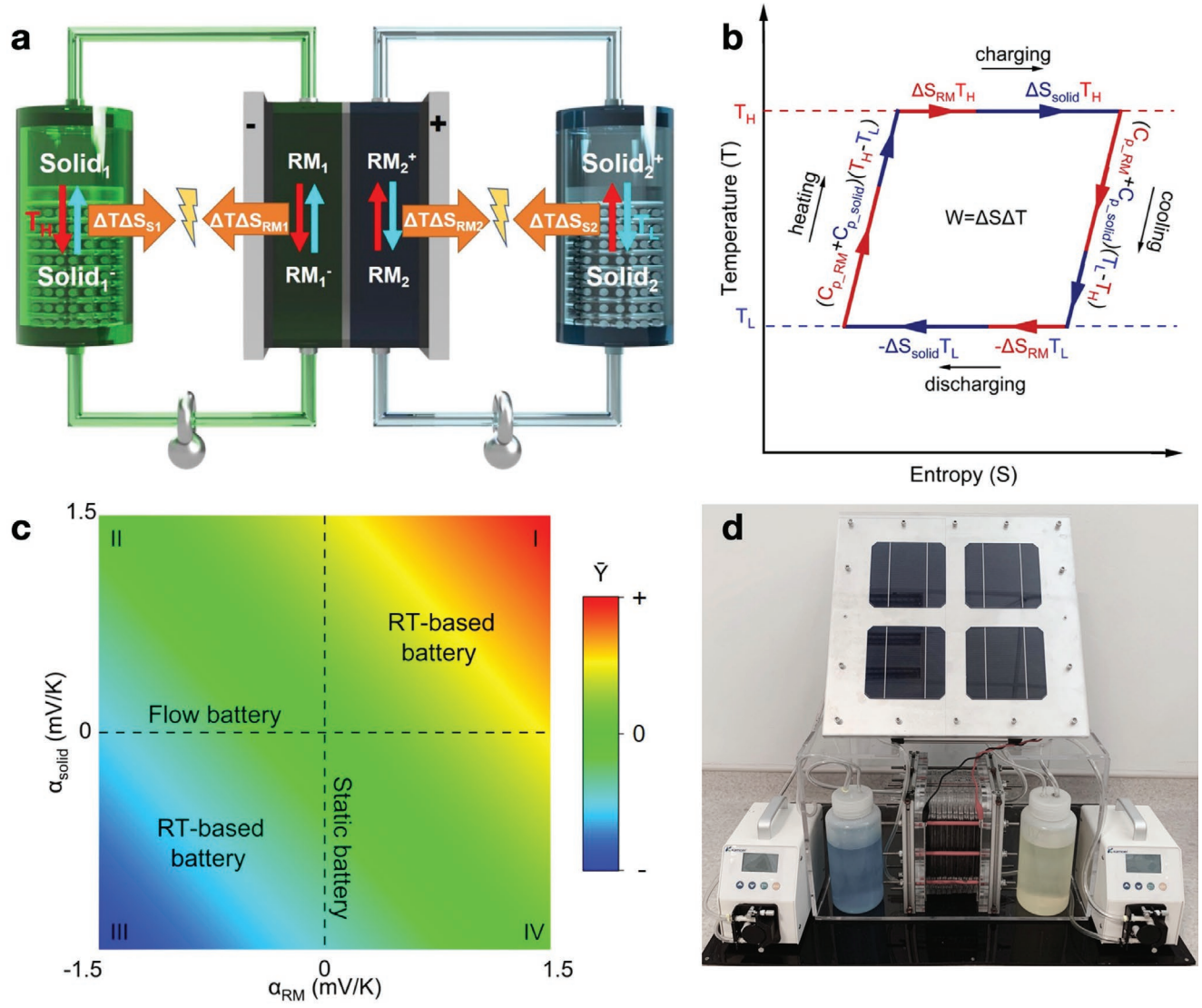

Figure 6. a) Schematic illustration of a RT-based TREC flow cell. b) Temperature–entropy (T–S) diagram of a RT-based flow cell during a full TREC cycle. c) Thermoelectric figure of merit ($\overline{Y}$) of the half-cell of a RT-based TREC flow cell at different temperature coefficient of the redox mediator in the electrolyte and solid active material in the tank. (a–c) Reproduced with permission.[13] Copyright 2021, Wiley-VCH. d) Photograph of a PV panel integrated with a RFB system for concurrent energy storage, cooling, and waste heat harnessing.

in each half-cell, RT reaction of soluble redox mediators in the electrolyte with solid energy materials in the tank incorporates solid and liquid phase thermal-to-electrical conversion in the same cell. As such, both contribute to the thermoelectrical process. As an example, solid active material $Ni_{0.2}Co_{0.8}(OH)_2$ and redox mediator $[Fe(CN)_6]^{4-/3-}$, both of which have negative temperature coefficient and share identical redox potentials, can be paired via the Nernstian potential-driven SMRT reaction to boost the capacity and entropy change during TREC process (Figure 6b). Compared with either TREC static cell using $Ni_{0.2}Co_{0.8}(OH)_2$ as the active material or flow cell using $[Fe(CN)_6]^{4-/3-}$ as the soluble redox species, the RT-based TREC flow cell has larger thermoelectric figure of merit (Figure 6c) and can thus achieve higher thermal-to-electrical efficiency. Such a RT-based TREC flow cell with an overall negative temperature coefficient could be integrated with PV panels for concurrent cooling (performance of Si PV degrades at elevated temperatures), on-site electricity storage, and waste heat harnessing (Figure 6d). In the daytime, the redox fluids flow through solar panels taking away the heat and injecting it to the flow cell, which enhances the power conversion efficiency of PV and raises the temperature of TREC cell (T_H). Meanwhile the generated solar electricity is stored in the flow cell by charging at a lower voltage. At night, when the temperature becomes lower (T_L), the flow cell is discharged to the grid at a higher cell voltage, during which additional electricity is produced from waste heat. Similarly, the RT-based system with positive temperature coefficient could be used for simultaneous cooling, powering, and waste heat harnessing for future computing.

4.2. RT-Based Solar-to-Electrical Energy Conversion

Due to the intermittent nature of solar illumination, the growing penetration of photovoltaics requires timely storage of the generated electricity in order to buffer its impact to the power grid. Integrating the photoelectrochemical conversion devices to RFBs is an interesting approach for simultaneous solar-to-electrical energy conversion and storage.[53] However, the concentrations of RMs vary during operation, which along with the low energy density of conventional RFB chemistries, set barriers to the practical use of these solar rechargeable flow batteries (SRFBs).[54] In 2017, Fan et al. reported an RT-based SRFB, which rationally mitigates the above problems.[47] Compared to RTFB, an additional sensitized TiO_2 photoelectrode was introduced to SRFB for light harvesting. In the reported system, PB was loaded in a tank as a low-cost Li^+-storage material to improve the energy density. During the photo-charging process, the dye molecules adsorbed on TiO_2 become photoexcited and inject the photogenerated electrons into the conduction band of TiO_2. Under external bias, the photogenerated electrons subsequently move to the lithium anode through external circuit. Meanwhile, I^- in the electrolyte captures holes from the highest occupied molecular orbital (HOMO) of dye molecules and is oxidized to I_3–, which subsequently oxidizes the Prussian white (PW) in the tank back to PB. Through the RT reaction between I^-/I_3^- and PB/PW, solar energy is constantly stored in the form of PB in the tank, during which the electrolyte retains a stable I^-/I_3^- concentration. This is crucial to the operation of SRFB. The discharge process is similar to other RTFBs, for which a second RM EV^{2+} in the catholyte is electrochemically reduced to EV^+ and it then reduces PB back to PW by the RT reaction. With such a RT process, the stored charges in PB are continuously released.

4.3. RT-Based Water Electrolysis for On-Demand Hydrogen Production

Hydrogen has the highest energy density by weight of all known fuels while without CO_2 emission, and is a crucial feedstock for the entire chemicals industry.[55] It must be produced from a hydrogen-containing feedstock (e.g., water, biomass, fossil fuels, or waste materials) using an energy source. The traditional electrical-to-hydrogen conversion is achieved by electrolytic water splitting which simultaneously produces H_2 and O_2 on the cathode and anode, respectively, separated by a membrane. While water electrolysis is an effective way to produce high purity H_2, the large-scale and continuous green H_2 production from the renewable energy sources still confronts challenges to surmount. For instance, it requires a means of electricity storage to buffer the intermittent electricity input for continuous and stable operation.[56] Furthermore, as the HER and OER are coupled both in time and space in traditional water electrolysis, it may induce gas mixing issue especially at high pressure or low operating current, which brings about compromised purity, system durability, and energy efficiency.[14b,c,57] In addition, the production rate of H_2 is limited by the sluggish reaction of OER process. To address these issues of conventional water electrolysis, RT process has been introduced for decoupled generation of H_2 and O_2.[14b,c,58] The system is similar to RFB while the electrolyte tanks are loaded with HER or OER catalysts. Such a design was first reported by Girault and co-workers. In their report, $V^{2+/3+}$ (–0.26 V vs SHE) and $Ce^{3+/4+}$ (1.44 V vs SHE) in sulfuric acid were used as cathodic and anodic RMs, respectively.[58a] As their potentials stay beyond the thermodynamic limit of water electrolysis but kinetically slow in the absence of catalysts, they can be electrochemically charged on the electrodes as normal RFBs, and then chemically discharged to produce H_2 and O_2 when they flow through catalyst tanks loaded with Mo_2C and RuO_2, respectively.

Recently, Zhang et al. has reported an alkaline system with considerably lower cell voltage, in which 7,8-dihydroxy-2-phenazinesulfonate (DHPS) and $[Fe(CN)_6]^{4-/3-}$ were employed as the HER and OER redox mediators, respectively (**Figure 7**a).[14b] As shown in Figure 7b, the potential of $[Fe(CN)_6]^{4-/3-}$ is 1.37 V (vs RHE), slightly higher than that of OER reaction (1.23 V vs RHE). It serves as an energetic charge carrier circulating between the electrode and $NiFe(OH)_2$ catalyst bed, during which the electrochemically generated $[Fe(CN)_6]^{3-}$ carries hole from the anode to the catalyst for OER reaction. For HER side, DHPS has a potential of –0.05 V (vs RHE) and served both as proton and electron carriers. It undergoes fast electrochemical hydrogenation reaction on the cathode forming DHPS-2H, and is then rapidly dehydrogenated to produce H_2 when flowing through a Pt catalyst bed in the tank (Figure 7e). Such a RT process through the electrochemical–chemical cycle between the electrode and

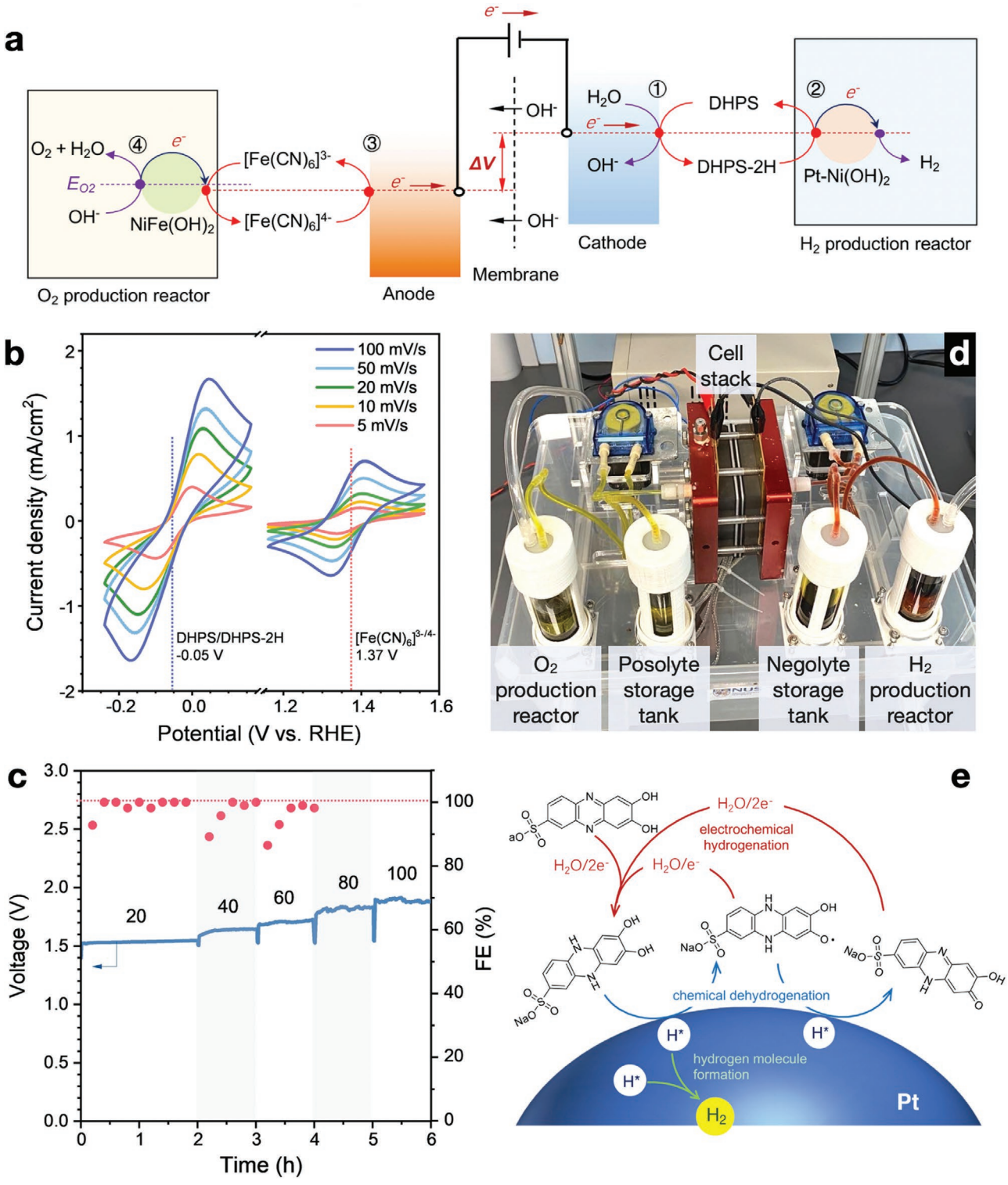

Figure 7. a) Energy diagram of electrolyte-borne redox-assisted HER and OER reactions with DHPS and ferricyanide as the mediators, respectively. A regenerative electrochemical–chemical cycle is applied on anodic and cathodic compartments, respectively, for continuous and concurrent O_2 and H_2 production. b) CV curves of 5 mM DHPS and $[Fe(CN)_6]^{4-/3-}$ in 4 M NaOH solution on a glassy carbon electrode at different scan rates. c) Voltage profile and H_2 production faradic efficiency of the electrolytic flow cell at different current densities. d) Photograph of the set up integrated with energy storage and decoupled on-demand H_2 production, consisting of a cell stack, two electrolyte tanks, and two reactor tanks. e) Proposed reaction mechanism of the stepwise chemical dehydrogenation process of DHPS-2H on Pt for H_2 formation and regenerative electrochemical hydrogenation process of DHPS on electrode. These form a close-loop electrochemical–chemical cycle for sustained and spatially decoupled H_2 generation. (a–c, e) Reproduced with permission.[14b] Copyright 2021, American Chemical Society.

catalyst reactor tank presents a fast, sustained, and decoupled production of H_2 (Figure 7c). Moreover, as the system with the pair of RMs could perform as a RFB in the absence of catalysts in the tanks, electricity storage and on-demand H_2 production could be concurrently accomplished (see the configuration consisting of two storage tanks plus two gas production reactors in Figure 7d).

4.4. RT-Based Electrolytic N_2 Reduction for Ammonia Production

The production of NH_3 from N_2 is among the most attractive and important topics in the field of chemistry.[59] The N_2 molecule is highly stable due to the extremely strong triple bond and large energy gap between its HOMO and LUMO.[60] Thanks to the Haber–Bosch process ingeniously invented in the early 20th century, people have doubled the amount of nitrogen available to living systems, which has fundamentally altered the global nitrogen cycle, revolutionized the production of food, and supported half of the world's population. As a result, NH_3 has become the second highest produced chemical in the world. However, the Haber–Bosch process requires a high temperature and high pressure for accelerated kinetics and favorable equilibrium for the reaction between N_2 and H_2.[61] The annual NH_3 production counts for 1–2% of global energy consumption, and utilization of half the global H_2 production which is largely based on transformations of fossil resources. N_2 reduction at ambient conditions has recently attracted intensive interest worldwide, not only for the fertilizer industry, but also for advanced energy systems – ammonia has a high energy density, thus is an ideal low-carbon energy carrier and storage medium for renewable energy sources, especially because it can be easily transported.[62] With extensive efforts made in the past few years, the ambient electrocatalytic nitrogen reduction reaction (eNRR) has witnessed substantial improvement for both NH_3 yield and faradaic efficiency. Nonetheless, the performance is still far from being practical compared with the Haber–Bosch process. Redox-mediated electrolytic nitrogen reduction reaction (RM-eNRR) using polyoxometalate (POM) as the electron and proton carrier was recently reported by Wang et al., in which the RM–eNRR proceeds on the surface of Fe–TiO_2 catalyst loaded in a reactor tank (see Figure 1b).[14d] The RM–eNRR process has achieved an ammonium production yield of 25.1 μg h^{-1} or 5.0 μg h^{-1} cm^{-2} at an ammonium concentration of 6.7 ppm. With a high catalyst loading, 61.0 ppm ammonium was accumulated in the electrolyte upon continuous operation, which is the highest concentration detected for ambient eNRR so far. The mechanism underlying the RM-eNRR was scrutinized both experimentally and computationally, which revealed a stepwise POM-mediated charge transfer and hydrogenation process of N_2 on the catalyst. RM–eNRR is expected to provide an implementable solution to overcome the limitations in the conventional eNRR process, where the reaction is constrained by the sluggish charge transfer kinetics and N_2 mass transport at the electrode/electrolyte interface.

Compared with the conventional energy conversion processes, RT-based systems could be directly integrated with RFBs for both distributed energy conversion and on-demand chemical synthesis. Such an operation flexibility however relies on sophisticated system design with optimized electrolyte flow, reactants feeding and catalyst loading, so that fast while balanced electrochemical and catalytic reactions are achieved. These systems also face several challenges as RFBs, such as the chemical stability of RMs, side reactions, and electrolyte crossover, which may impede their operation stability and conversion efficiency, especially when operated in strong acid or alkaline media or at elevated temperatures. Moreover, the catalyst bed plays a critical role in the RT-based catalytic reactions. A rational design of the loading of suitable catalysts with maximized reaction sites, facilitated mass transport for both the redox species and gaseous reactants (if any), and fast removal of products is desired. With the decoupled design, sometimes additional energy input, such as thermal and photo energy, could even be introduced to the reactor tank to overcome the kinetic limitations related to the intrinsic barriers for the formation of intermediates and transition states especially for some multi-protons and multi-electrons involved reactions. This provides additional flexibility for promoting the reaction kinetics. In addition, the distinct reaction pathway of the redox-assisted catalytic reactions may create interesting opportunities for low-cost catalysts, which could be loaded in greater surface area given the ample space in the reactor tanks compared with that on electrode surface.

5. RT Process for Other Applications

Apart from the aforementioned energy storage and conversion applications, the RT process, for which the solid functional material and electrode stay spatially separated while electrically wired via a regenerative electrochemical–chemical cycle of redox mediator, has versatile intriguing applications in other fields, such as hydrometallurgical mineral extraction,[63] electrochromic windows,[64] and spent battery materials recycling.[65] Currently, the industrially implemented recycling technologies of spent Li-ion batteries are primarily pyrometallurgy and hydrometallurgy. The former involves using high temperatures to smelt the metals and burn away the remaining components like carbon and separators. The formed metal alloy is then treated by hydrometallurgy to obtain various salts. But the pyrometallurgical process, despite being simple and requiring no extra-sorting and pre-processing, uses a huge amount of energy and generates a large amount of toxic and CO_2 gases. In comparison, the hydrometallurgical process involves leaching the elements from cathode materials and then recovering them either by solvent extraction or salt precipitation. The main advantages of the process are that it recovers a high proportion of the battery elements and does not require a huge amount of energy. However, the leaching process is tedious and consumes large quantities of hazardous chemicals. Inevitably, it introduces secondary pollutions. In 2019, Yu et al. reported a novel RT-based electrolytic flow cell system to continuously recycle spent battery materials into valuable chemicals at ambient conditions, without consuming additional chemicals (**Figure 8**a).[65] Upon operation, spent $LiFePO_4$ is rapidly broken down to solid $FePO_4$ and soluble Li^+ via the RT reaction with $[Fe(CN)_6]^{3-}$ in the anolyte. The reacted redox species

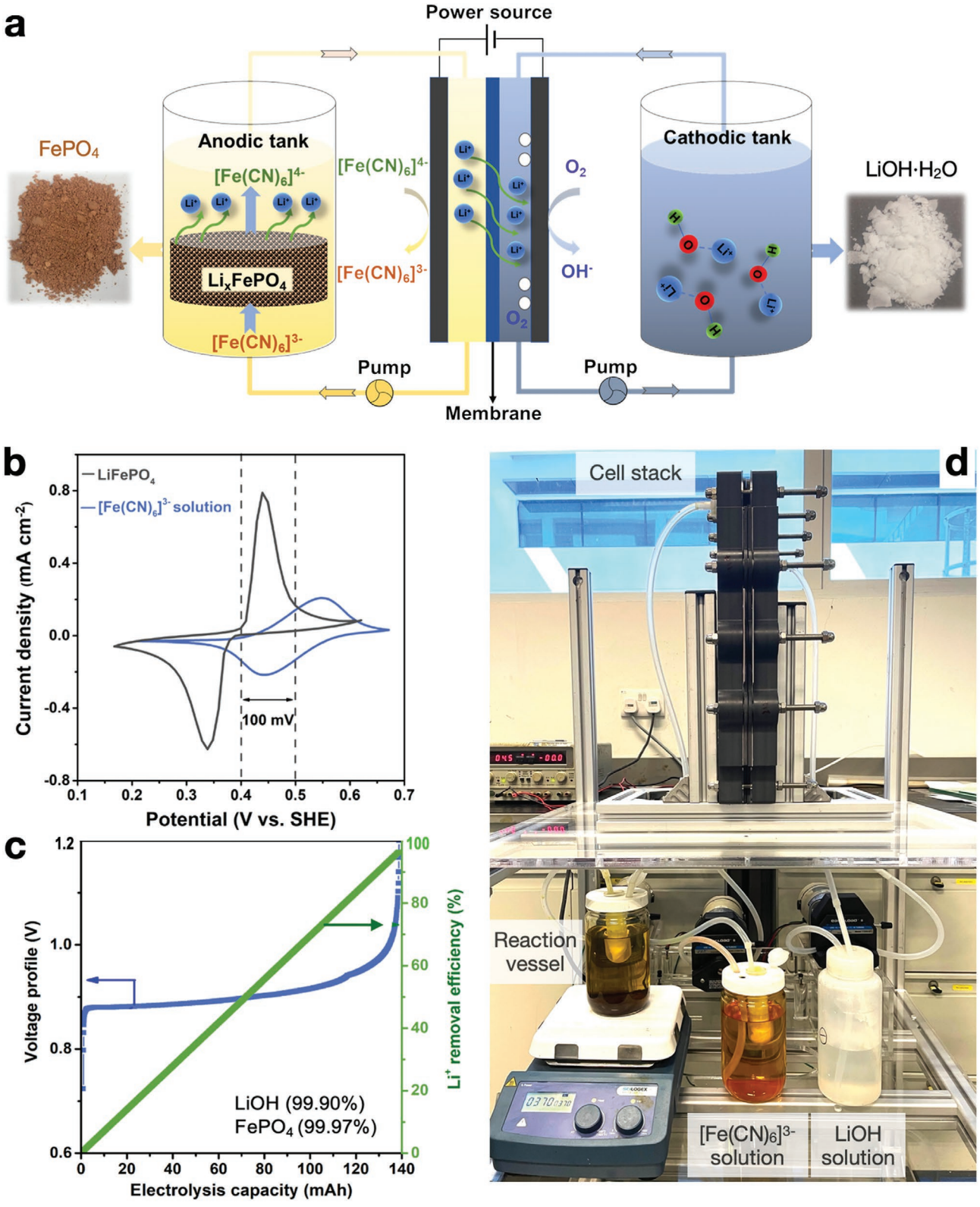

Figure 8. a) Illustration of the regenerative RT-based recycling for spent $LiFePO_4$ material. It shows selective Li removal from the anodic tank, reagent regeneration in the cell, and Li^+ separation to the counter compartment. b) CV curves of $[Fe(CN)_6]^{4-/3-}$ and $LiFePO_4$ measured in 0.5 M Li_2SO_4 solution. (a,b) Reproduced with permission.[65] Copyright 2019, The Royal Society of Chemistry. c) Voltage profile of the flow cell loaded with 40 mL of 0.20 M $[Fe(CN)_6]^{3-}$ and 0.9 g of $LiFePO_4$ in the anodic tank, and 0.10 M LiOH solution bubbled with O_2 in the cathodic tank. The current density was 5 mA cm^{-2}. Adapted with permission.[65] Copyright 2019, The Royal Society of Chemistry. d) Photograph of a lab recycling setup, consisting of a 900 cm^2 cell stack, a reaction vessel, a catholyte tank, and a LiOH collection tank.

are instantaneously regenerated on the anode for subsequent round of reactions, while Li^+ is separated in the form of LiOH from the cathode compartment through an ORR reaction (overall reaction: $LiFePO_4 + 1/4O_2 + 1/2H_2O \rightarrow FePO_4 + LiOH$). Consequently, chemical consumption is drastically minimized. With $[Fe(CN)_6]^{4-/3-}$ as a regenerative redox couple, a recycling efficiency for Li removal as high as 99.8% has been achieved at room temperature, and high purity LiOH (99.90%) and $FePO_4$ (99.97%) are obtained through the RT process (Figure 8b,c). This approach eliminates the massive consumption of chemicals and consequently the secondary pollution compared with the conventional recycling technologies. In addition, the electrolytic flow cell design makes the system readily scalable to large size (Figure 8d). With suitable redox chemistry and counter electrode reactions, it is anticipated that this environment-friendly and cost-effective approach can be extended for the recycling of other spent battery materials.

6. Challenges and Perspective

The above sections have shown a wide variety of RT-based processes via regenerative electrochemical–chemical cycles for diversified energy storage and conversion applications. With the assistance of redox mediators shuttling between the electrode compartment and reactor tank, not only is the border of the conventional electrochemical reaction spatially extended beyond the electrode compartment, but the system is also endowed with salient features for various innovative applications. These new attributes are distinct and manifold, in addition to those previously summarized.[19] The prevailing one-step electrochemical reaction in the conventional system is split into a spatially decoupled two-step electrochemical–chemical process, which provides the system with great flexibility for various real-time or even operando spectroelectrochemical characterizations of both the RMs and solid active materials, such as X-ray absorption spectroscopy, UV–vis spectroscopy, and FTIR spectroscopy measurements as those depicted in **Figure 9**. Dependent on the techniques, an optical cell transparent to the detection signals is connected to the outlet flow channel of a flow cell, and the property changes (i.e., concentration, bond, valence state, chemical environment, etc.) of RMs in the electrolyte and solid materials loaded in the cell are monitored, with which the underlying RT reaction mechanism is deciphered and a clear picture of the RT reactions between the RMs and solid materials at different stages of operation, is delineated.

While the RT process is poised to bring significant advantages to various electrochemical energy storage and conversion systems, the following are required to be adequately addressed before it becomes a credible and viable reality for practical applications: (1) judiciously developed redox chemistry and materials; (2) vigorous engineering design and system level optimization; (3) rational membrane selection and optimization.

A wide variety of RMs and solid active materials have been demonstrated for RT-based energy storage and conversion applications. These diversified RT processes involve not only simple charge transfer of RMs on electrode or with the solid active materials in reactor tank, but also are frequently coupled with other species in the system. For instance, the RMs serve both as electron and proton carriers and are part of the proton-coupled charge transfer processes, as those revealed in RT-based water splitting and N_2 reduction processes.[14b–d] For other systems, the RT reaction may involve guest species such as Li^+ and the reaction may be limited by the transport of these species.[27] So, the intricacies of these RT reactions require judicious design of the redox chemistry and associated materials adapted to a specific reaction or process. In addition, the cycling stability of redox species is also of paramount importance for the various energy applications, for which the RMs and solid active materials are required to undergo repeated reactions. Considering the RMs act as mediators shuttling between the electrode and solid materials, the actual turnovers of RMs would be considerably more than the cycle numbers of device operation.

Due to the critical requirement for potential matching, the choices of RMs with high solubility, stability, and fast reaction kinetics are seemingly limited, especially when focused on the exhaustively studied inorganic species. However, the highly customizable organic redox species provide immense possibilities for searching suitable RMs. For instance, organic derivatives of quinone,[66] alloxazine,[67] phenazine,[68] viologen,[69] fluorenone,[70] and TEMPO[71] covering a broad range of redox potentials and pH, have been extensively studied. The electrochemical characteristics of organic RMs can be tailored and modified on account of their ample structural diversity and tunability.[3a,72] Different strategies of molecular engineering have been applied to increase the solubility, adjust the redox potential, and ensure the chemical integrity of these molecules via ingenious synthetic routes.[73] In addition, supporting electrolytes and co-solvents have been shown to play an important role in tuning the above properties. Moreover, it has been suggested that the structural similarity between the soluble RMs and solid active material may facilitate the reaction kinetics of SMRT. This has been applied to some open structured materials such as redox active polymers,[74] covalent–organic frameworks and metal–organic frameworks compounds where the building blocks are made of redox active species of similar structures.[1a,75] Besides extensive experimental studies, high throughput computations, including DFT and molecular dynamics simulations, and machine learning, are also useful in the screening of suitable RMs by estimating the potential shift, solubility and stability with the introduced functional groups and changes in surrounding electrolyte conditions.[76]

In addition to materials development, the reactor tank loaded with solid active materials (energy storage material or catalyst) working as a packed-bed reactor, is another crucial part of the system. The RT reactions inside the reactor tank essentially dictate the operation of the system. There are generally multiple kinetic processes involved in the tank at different length scales.[19] These multiple-step processes significantly impact the performance for various energy applications. For instance, material utilization, cycling performance, and system maintenance would be critically influenced by the tank design and loading of solid materials. The materials in the tank are usually processed into pellets or granules for dense packing and

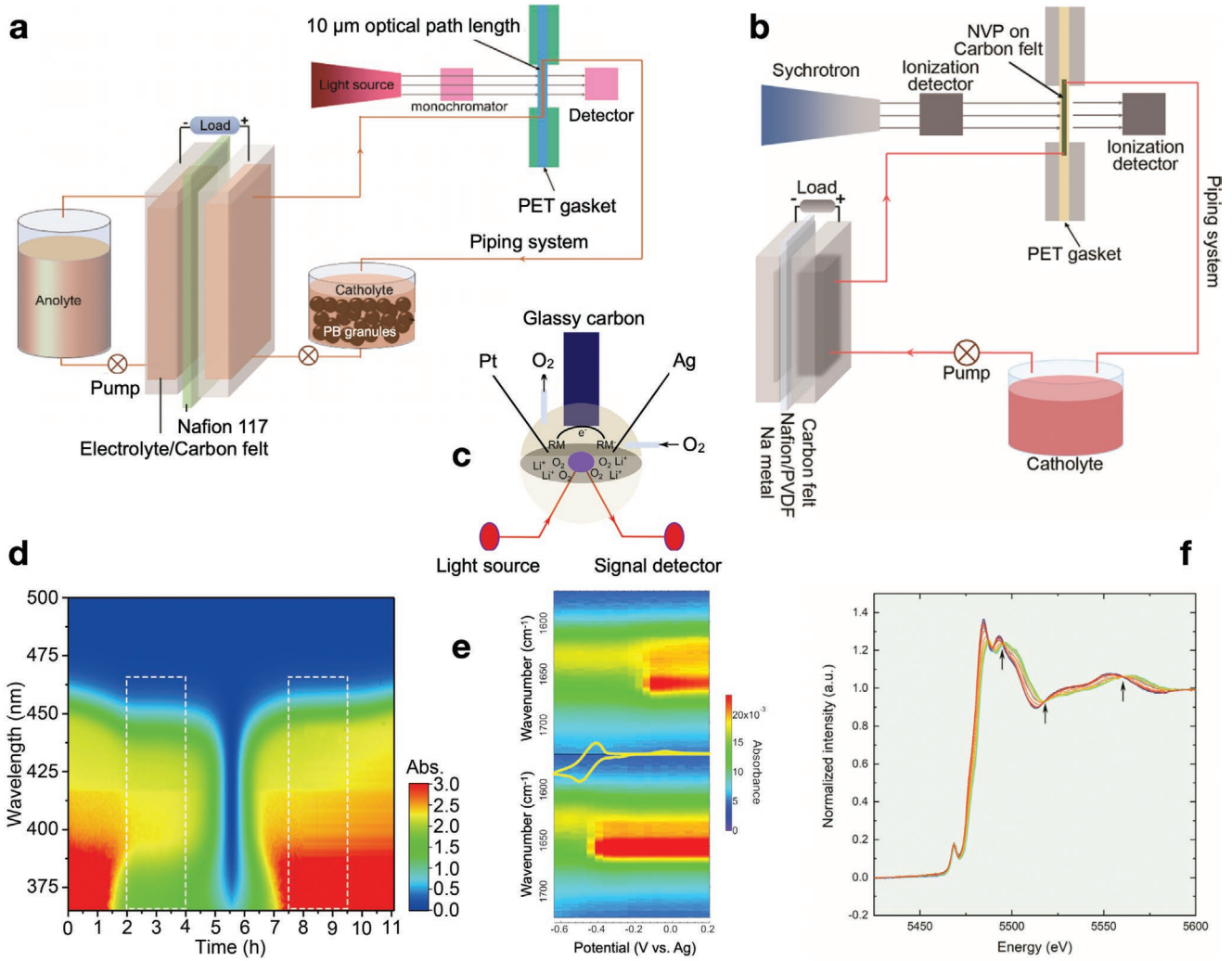

Figure 9. a) Configuration of the setup for operando UV–vis measurement. b) A two-body setup for operando X-ray absorption near-edge structure (XANES) experiment. c) Schematic of an in situ spectroelectrochemical FTIR cell. d) Operando UV–vis spectra of the catholyte of a PB-loaded symmetric flow cell at different durations of charge/discharge. e) FTIR spectra of f) Selected X-ray near edge absorption spectra of vanadium in NVP. The arrows indicate the isosbestic points. (a,d) Reproduced with permission.[36] Copyright 2019, Elsevier. (b,f) Reproduced with permission.[32] Copyright 2019, Wiley-VCH. (c,e) Adapted with permission.[46] Copyright 2018, The Royal Society of Chemistry.

convenient handling (see Figure 4d), while the structural properties of the granules, such as the shape, size, porosity, and tortuosity, determine the diffusion pathway, reaction rate, and the material utilization.[19] In addition, the flow patterns of the electrolyte through the solid materials also play an important role during operation. A good "filtering" effect of the redox electrolyte flowing through the material without "dead" volume would ensure a large contact area and maximize the utilization. But it may also induce a larger flow resistance and increase the pumping power, especially with a high loading of solid materials. For those involving gaseous phase, the feed of gaseous reactant along with electrolyte flow would be equally important for fast RT reactions. Since each variable of the above parameters affects the device performance in different ways, a systematic study of the engineering design and system optimization are desired in the next stage. Moreover, computer modeling would be a useful tool to efficiently investigate the fluid dynamics of the electrolyte (flow distribution and pressure drop, etc.) and mass transport of RMs within the solid phase, which will provide important guidance to the optimization of reactor tank and consequently the performance of entire system.[77]

Last but not the least, another critical component is the membrane which separates the cathodic and anodic compartments while facilitating the passage of charge balancing ions. An ideal membrane should have high ionic conductivity, high selectivity, excellent chemical stability, and mechanical robustness in various electrolytes upon prolonged operation. The membranes for non-aqueous systems however have the major obstacles of sluggish ion transport (i.e., Li^+ and Na^+) and swelling of the polymeric membranes by organic solvents. For aqueous systems, Nafion series cation-exchange membranes are most widely used in electrolytes of full pH range. However, their high cost and low ion selectivity are barriers for large-scale

deployment. Anion-exchange membranes are interesting options for neutral or alkaline media, while the conductivity and durability of the commercial products are not on par with their cation-exchange counterpart.[78] In addition, the selection of membrane has to consider the fouling effect which is frequently observed while rarely reported in RFBs involving redox species possessing the same charge as the counterions of membrane and having a large partition coefficient, and has profound impact to the device performance. These charged redox species accumulate inside the membrane and at the membrane/electrolyte interface, blocking the ion-exchange sites in the membrane and creating an electric field at the interface inhibiting ion transport. Overall, the rational selection and optimization of membrane dependent on the RMs and supporting electrolyte are indispensable to the high-performance RT-based energy storage and conversion devices.

7. Summary

We have summarized the recent progress in the RT-based processes for various energy storage and conversion applications. The two-step regenerative electrochemical–chemical process between soluble RMs and solid active materials extends the border of conventional electrochemical reactions beyond the electrode compartment to a new frontier, at which various advanced energy-related processes have been realized. As the many examples revealed, integrating the RT processes with redox-flow cells provides a promising approach to surmount the critical limitations inherently confronted by conventional electrochemical systems. For RT-based energy storage, leveraging the redox-mediated reactions of RMs with charge storage materials in the tank, the system elegantly circumvents the solubility limits of redox electrolytes and breaks the boundary of solid and liquid phase energy storage, and as a result presents unprecedented energy density for large-scale applications. For RT-based energy conversion and chemical productions, the close-loop electrochemical–chemical processes enable the system with extended reaction sites in the reactor tank, which overcomes the space constraints of the electrode compartment for enhanced reaction yield. Among many other interesting applications and given the salient features demonstrated as compared to the conventional systems, we anticipate the concept of redox targeting of energy material based upon a regenerative electrochemical–chemical cycle will provide an intriguing platform, based on which important energy-related studies are incubated and grow into credible and viable solutions to the grand energy and sustainability issues.

Acknowledgements

This research is supported by the National Research Foundation, Prime Minister's Office, Singapore under its Investigatorship Programme (Award No. NRF-NRFI2018-06).

Conflict of Interest

The authors declare no conflict of interest.

Keywords

energy storage and conversion, redox flow batteries, redox-mediated process, redox-targeting process

Received: June 14, 2021
Revised: August 13, 2021
Published online:

[1] a) L. Kong, M. Zhong, W. Shuang, Y. Xu, X.-H. Bu, *Chem. Soc. Rev.* **2020**, *49*, 2378; b) X. Li, J. Wang, *InfoMat* **2019**, *2*, 3; c) P. J. McHugh, A. D. Stergiou, M. D. Symes, *Adv. Energy Mater.* **2020**, *10*, 2002453.

[2] a) T. N. Pham-Truong, Q. Wang, J. Ghilane, H. Randriamahazaka, *ChemSusChem* **2020**, *13*, 2142; b) Y. Yao, J. Lei, Y. Shi, F. Ai, Y.-C. Lu, *Nat. Energy* **2021**, *6*, 582; c) D. R. MacFarlane, P. V. Cherepanov, J. Choi, B. H. R. Suryanto, R. Y. Hodgetts, J. M. Bakker, F. M. Ferrero Vallana, A. N. Simonov, *Joule* **2020**, *4*, 1186.

[3] a) J. Luo, B. Hu, M. Hu, Y. Zhao, T. L. Liu, *ACS Energy Lett.* **2019**, *4*, 2220; b) L. Li, S. Kim, W. Wang, M. Vijayakumar, Z. Nie, B. Chen, J. Zhang, G. Xia, J. Hu, G. Graff, J. Liu, Z. Yang, *Adv. Energy Mater.* **2011**, *1*, 394; c) W. Yan, C. Wang, J. Tian, G. Zhu, L. Ma, Y. Wang, R. Chen, Y. Hu, L. Wang, T. Chen, J. Ma, Z. Jin, *Nat. Commun.* **2019**, *10*, 2513.

[4] a) J.-B. Tan, G.-R. Li, *J. Mater. Chem. A* **2020**, *8*, 14326; b) M. I. Jamesh, Y. Kuang, X. Sun, *ChemCatChem* **2019**, *11*, 1550; c) B. Wu, H. Qian, Z. Nie, Z. Luo, Z. Wu, P. Liu, H. He, J. Wu, S. Chen, F. Zhang, *J. Energy Chem.* **2020**, *46*, 178; d) Y. Peng, K. Jiang, W. Hill, Z. Lu, H. Yao, H. Wang, *ACS Appl. Mater. Interfaces* **2019**, *11*, 3971.

[5] a) Y. Yang, S. W. Lee, H. Ghasemi, J. Loomis, X. Li, D. Kraemer, G. Zheng, Y. Cui, G. Chen, *Proc. Natl. Acad. Sci U.S.A.* **2014**, *111*, 17011; b) B. Yu, J. Duan, H. Cong, W. Xie, R. Liu, X. Zhuang, H. Wang, B. Qi, M. Xu, Z. L. Wang, J. Zhou, *Science* **2020**, *370*, 342; c) S. W. Lee, Y. Yang, H. W. Lee, H. Ghasemi, D. Kraemer, G. Chen, Y. Cui, *Nat. Commun.* **2014**, *5*, 3942.

[6] X. Wang, M. Zhou, F. Zhang, H. Zhang, Q. Wang, *Curr. Opin. Electrochem.* **2021**, *29*, 100743.

[7] H. Wei, D. Cui, J. Ma, L. Chu, X. Zhao, H. Song, H. Liu, T. Liu, N. Wang, Z. Guo, *J. Mater. Chem. A* **2017**, *5*, 1873.

[8] a) Y. Zhu, F. W. T. Goh, Q. Wang, *Nano Mater. Sci.* **2019**, *1*, 173; |b) Y. G. Zhu, X. Wang, C. Jia, J. Yang, Q. Wang, *ACS Catal.* **2016**, *6*, 6191.

[9] a) Z. Li, Y. C. Lu, *Adv. Mater.* **2020**, *32*, 2002132; b) Y. Ding, C. Zhang, L. Zhang, Y. Zhou, G. Yu, *Chem. Soc. Rev.* **2018**, *47*, 69.

[10] a) Q. Wang, S. M. Zakeeruddin, D. Wang, I. Exnar, M. Grätzel, *Angew. Chem., Int. Ed.* **2006**, *118*, 8377; b) Q. Wang, N. Evans, S. M. Zakeeruddin, I. Exnar, M. Gratzel, *J. Am. Chem. Soc.* **2007**, *129*, 3163.

[11] Q. Huang, H. Li, M. Grätzel, Q. Wang, *Phys. Chem. Chem. Phys.* **2013**, *15*, 1793.

[12] a) Q. Huang, Q. Wang, *ChemPlusChem* **2015**, *80*, 312; b) F. Pan, Q. Wang, *Molecules* **2015**, *20*, 20499; c) X. Wang, J. Chai, J. J. Jiang, *Nano Mater. Sci.* **2021**, *3*, 17.

[13] H. Zhang, F. Zhang, J. Yu, M. Zhou, W. Luo, Y. M. Lee, M. Si, Q. Wang, *Adv. Mater.* **2021**, *33*, 2006234.

[14] a) Y. Ji, F. Zhang, M. Zhou, J. Yu, Q. Wang, *Int. J. Hydrog. Energy* **2020**, *45*, 18888; b) F. Zhang, H. Zhang, M. Salla, N. Qin, M. Gao, Y. Ji, S. Huang, S. Wu, R. Zhang, Z. Lu, Q. Wang, *J. Am. Chem. Soc.* **2021**, *143*, 223; c) F. Zhang, Q. Wang, *ACS Mater. Lett.* **2021**, *3*, 641; d) X. Wang, J. Yang, M. Salla, S. Xi, Y. Yang, M. Li, F. Zhang, M. Zhu, S. Huang, S. Huang, Y. Zhang, Q. Wang, *Angew. Chem., Int. Ed.* **2021**, *60*, 18721.

[15] a) T. Kwon, M. Jun, K. Lee, *Adv. Mater.* **2020**, *32*, 2001345; b) H. Han, Z. Bai, T. Zhang, X. Wang, X. Yang, X. Ma, Y. Zhang, L. Yang, J. Lu, *Nano Energy* **2019**, *56*, 724.
[16] a) P. Trogadas, M. O. Coppens, *Chem. Soc. Rev.* **2020**, *49*, 3107; b) M. Gao, S. Huang, F. Zhang, Y. M. Lee, S. Huang, Q. Wang, *Mater. Today Energy* **2020**, *18*, 100540; c) F. Zhang, S. Huang, X. Wang, C. Jia, Y. Du, Q. Wang, *Nano Energy* **2018**, *52*, 292.
[17] J. Nai, X. W. D. Lou, *Adv. Mater.* **2018**, *31*, 1706825.
[18] J. Yu, M. Salla, H. Zhang, Y. Ji, F. Zhang, M. Zhou, Q. Wang, *Energy Storage Mater.* **2020**, *29*, 216.
[19] R. Yan, Q. Wang, *Adv. Mater.* **2018**, *30*, 1802406.
[20] a) Q. Huang, Q. Wang, *Chin. Phys. B* **2015**, *25*, 018213; b) F. Pan, J. Yang, C. Jia, H. Li, Q. Wang, *J. Energy Chem.* **2018**, *27*, 1362.
[21] F. Pan, J. Yang, Q. Huang, X. Wang, H. Huang, Q. Wang, *Adv. Energy Mater.* **2014**, *4*, 1400567.
[22] C. Jia, F. Pan, Y. G. Zhu, Q. Huang, L. Lu, Q. Wang, *Sci. Adv.* **2015**, *1*, e1500886.
[23] J. R. Jennings, Q. Huang, Q. Wang, *J. Phys. Chem. C* **2015**, *119*, 17522.
[24] E. C. Self, F. M. Delnick, R. E. Ruther, S. Allu, J. Nanda, *ACS Energy Lett.* **2019**, *4*, 2593.
[25] C. M. Wong, C. S. Sevov, *ACS Energy Lett.* **2021**, *6*, 1271.
[26] a) D. G. Kwabi, Y. Ji, M. J. Aziz, *Chem. Rev.* **2020**, *120*, 6467; b) B. Hu, C. DeBruler, Z. Rhodes, T. L. Liu, *J. Am. Chem. Soc.* **2017**, *139*, 1207; c) Y. Zhao, Y. Ding, J. Song, G. Li, G. Dong, J. B. Goodenough, G. Yu, *Angew. Chem., Int. Ed.* **2014**, *53*, 11036.
[27] R. Yan, J. Ghilane, K. C. Phuah, T. N. Pham Truong, S. Adams, H. Randriamahazaka, Q. Wang, *J. Phys. Chem. Lett.* **2018**, *9*, 491.
[28] J. Yu, M. Salla, H. Zhang, Y. Ji, F. Zhang, M. Zhou, Q. Wang, *Energy Storage Mater.* **2020**, *29*, 216.
[29] F. Pan, Q. Huang, H. Huang, Q. Wang, *Chem. Mater.* **2016**, *28*, 2052.
[30] a) Q. Huang, J. Yang, C. B. Ng, C. Jia, Q. Wang, *Energy Environ. Sci.* **2016**, *9*, 917; b) Y. G. Zhu, Y. Du, C. Jia, M. Zhou, L. Fan, X. Wang, Q. Wang, *J. Am. Chem. Soc.* **2017**, *139*, 6286.
[31] a) E. Zanzola, C. R. Dennison, A. Battistel, P. Peljo, H. Vrubel, V. Amstutz, H. H. Girault, *Electrochim. Acta* **2017**, *235*, 664; b) M. Zhou, Q. Huang, T. N. P. Truong, J. Ghilane, Y. G. Zhu, C. Jia, R. Yan, L. Fan, H. Randriamahazaka, Q. Wang, *Chem* **2017**, *3*, 1036.
[32] M. Zhou, Y. Chen, Q. Zhang, S. Xi, J. Yu, Y. Du, Y. S. Hu, Q. Wang, *Adv. Energy Mater.* **2019**, *9*, 1901188.
[33] M. Zhou, Y. Chen, M. Salla, H. Zhang, X. Wang, S. R. Mothe, Q. Wang, *Angew. Chem., Int. Ed.* **2020**, *59*, 14286.
[34] Y. Zhou, G. Cong, H. Chen, N.-C. Lai, Y.-C. Lu, *ACS Energy Lett.* **2020**, *5*, 1732.
[35] J. Yu, L. Fan, R. Yan, M. Zhou, Q. Wang, *ACS Energy Lett.* **2018**, *3*, 2314.
[36] Y. Chen, M. Zhou, Y. Xia, X. Wang, Y. Liu, Y. Yao, H. Zhang, Y. Li, S. Lu, W. Qin, *Joule* **2019**, *3*, 2255.
[37] Y. Cheng, X. Wang, S. Huang, W. Samarakoon, S. Xi, Y. Ji, H. Zhang, F. Zhang, Y. Du, Z. Feng, *ACS Energy Lett.* **2019**, *4*, 3028.
[38] E. Zanzola, S. Gentil, G. Gschwend, D. Reynard, E. Smirnov, C. R. Dennison, H. H. Girault, P. Peljo, *Electrochim. Acta* **2019**, *321*, 134704.
[39] T. Páez, A. Martínez-Cuezva, J. Palma, E. Ventosa, *ACS Appl. Energy Mater.* **2019**, *2*, 8328.
[40] a) J.-S. Lee, S. T. Kim, R. Cao, N.-S. Choi, M. Liu, K. T. Lee, J. Cho, *Adv. Energy Mater.* **2011**, *1*, 34; b) Y.-C. Lu, B. M. Gallant, D. G. Kwabi, J. R. Harding, R. R. Mitchell, M. S. Whittingham, Y. Shao-Horn, *Energy Environ. Sci.* **2013**, *6*, 750; c) P. G. Bruce, S. A. Freunberger, L. J. Hardwick, J.-M. Tarascon, *Nat. Mater.* **2012**, *11*, 19; d) Y. G. Zhu, Q. Liu, Y. Rong, H. Chen, J. Yang, C. Jia, L. J. Yu, A. Karton, Y. Ren, X. Xu, S. Adams, Q. Wang, *Nat. Commun.* **2017**, *8*, 14308.
[41] T. Ogasawara, A. Débart, M. Holzapfel, P. Novák, P. G. Bruce, *J. Am. Chem. Soc.* **2006**, *128*, 1390.
[42] Y. Chen, S. A. Freunberger, Z. Peng, O. Fontaine, P. G. Bruce, *Nat. Chem.* **2013**, *5*, 489.
[43] F. Cheng, J. Chen, *Chem. Soc. Rev.* **2012**, *41*, 2172.
[44] H.-D. Lim, H. Song, J. Kim, H. Gwon, Y. Bae, K.-Y. Park, J. Hong, H. Kim, T. Kim, Y. H. Kim, X. Lepró, R. Ovalle-Robles, R. H. Baughman, K. Kang, *Angew. Chem., Int. Ed.* **2014**, *53*, 3926.
[45] Y. G. Zhu, C. Jia, J. Yang, F. Pan, Q. Huang, Q. Wang, *Chem. Commun.* **2015**, *51*, 9451.
[46] Y. G. Zhu, F. W. T. Goh, R. Yan, S. Wu, S. Adams, Q. Wang, *Phys. Chem. Chem. Phys.* **2018**, *20*, 27930.
[47] L. Fan, C. Jia, Y. G. Zhu, Q. Wang, *ACS Energy Lett.* **2017**, *2*, 615.
[48] a) F. Wang, W. Li, R. Wang, T. Guo, H. Sheng, H.-C. Fu, S. S. Stahl, S. Jin, *Joule* **2021**, *5*, 149; b) C. W. Anson, S. S. Stahl, *Chem. Rev.* **2020**, *120*, 3749; c) R. Francke, R. D. Little, *Chem. Soc. Rev.* **2014**, *43*, 2492; d) E. Steckhan, *Top. Curr. Chem.* **1987**, *142*, 1.
[49] L. E. Bell, *Science* **2016**, *321*, 1457.
[50] H. Zhang, Q. Wang, *Chem. Phys. Rev.* **2021**, *2*, 021304.
[51] C. Gao, S. W. Lee, Y. Yang, *ACS Energy Lett.* **2017**, *2*, 2326.
[52] D. Reynard, C. R. Dennison, A. Battistel, H. H. Girault, *J. Power Sources* **2018**, *390*, 30.
[53] a) K. Wedege, J. Azevedo, A. Khataee, A. Bentien, A. Mendes, *Angew. Chem., Int. Ed.* **2016**, *55*, 7142; b) S. Liao, X. Zong, B. Seger, T. Pedersen, T. Yao, C. Ding, J. Shi, J. Chen, C. Li, *Nat. Commun.* **2016**, *7*, 11474.
[54] Z. Yu, M. Gorlov, J. Nissfolk, G. Boschloo, L. Kloo, *J. Phys. Chem. C* **2010**, *114*, 10613.
[55] A. J. Hackett, J. Malmström, J. Travas-Sejdic, *ACS Appl. Energy Mater.* **2019**, *2*, 1436.
[56] B. M. H. Weninger, F. M. Mulder, *ACS Energy Lett.* **2019**, *4*, 567.
[57] a) A. Angulo, P. van der Linde, H. Gardeniers, M. Modestino, D. F. Rivas, *Joule* **2020**, *4*, 555; b) P. Belleville, F. Guillet, A. Pons, J. Deseure, G. Merlin, F. Druart, J. Ramousse, E. Grindler, *Int. J. Hydrogen Energy* **2018**, *43*, 14867.
[58] a) V. Amstutz, K. E. Toghill, F. Powlesland, H. Vrubel, C. Comninellis, X. Hu, H. H. Girault, *Energy Environ. Sci.* **2014**, *7*, 2350; b) D. Reynard, G. Bolik-Coulon, S. Maye, H. H. Girault, *Chem. Eng. Sci.* **2021**, *407*, 126721; c) P. Peljo, H. Vrubel, V. Amstutz, J. Pandard, J. Morgado, A. Santasalo-Aarnio, D. Lloyd, F. Gumy, C. R. Dennison, K. E. Toghill, H. H. Girault, *Green Chem.* **2016**, *18*, 1785; d) C. R. Dennison, H. Vrubel, V. Amstutz, P. Peljo, K. E. Toghill, H. H. Girault, *Chimia (Aarau)* **2015**, *69*, 753.
[59] a) A. Valera-Medina, H. Xiao, M. Owen-Jones, W. I. F. David, P. J. Bowen, *Prog. Energy Combust. Sci.* **2018**, *69*, 63; b) C. Tang, S. Z. Qiao, *Chem. Soc. Rev.* **2019**, *48*, 3166.
[60] a) L. Hu, Z. Xing, X. Feng, *ACS Energy Lett.* **2020**, *5*, 430; b) J. G. Chen, R. M. Crooks, L. C. Seefeldt, K. L. Bren, R. M. Bullock, M. Y. Darensbourg, P. L. Holland, B. Hoffman, M. J. Janik, A. K. Jones, M. G. Kanatzidis, P. King, K. M. Lancaster, S. V. Lymar, P. Pfromm, W. F. Schneider, R. R. Schrock, *Science* **2018**, *360*, eaar6611.
[61] X. Wang, M. Luo, J. Lan, M. Peng, Y. Tan, *Adv. Mater.* **2021**, *33*, 2007733.
[62] J. Choi, B. H. R. Suryanto, D. Wang, H. L. Du, R. Y. Hodgetts, F. M. Ferrero Vallana, D. R. MacFarlane, A. N. Simonov, *Nat. Commun.* **2020**, *11*, 5546.
[63] K. M. Deen, E. Asselin, *ChemSusChem* **2018**, *11*, 1533.
[64] R. Yan, L. Liu, H. Zhao, Y. G. Zhu, C. Jia, M. Han, Q. Wang, *J. Mater. Chem. C* **2016**, *4*, 8997.
[65] J. Yu, X. Wang, M. Zhou, Q. Wang, *Energy Environ. Sci.* **2019**, *12*, 2672.
[66] a) K. Lin, Q. Chen, M. R. Gerhardt, L. Tong, S. B. Kim, L. Eisenach, A. W. Valle, D. Hardee, R. G. Gordon, M. J. Aziz, *Science* **2015**, *349*, 1529; b) B. Huskinson, M. P. Marshak, C. Suh, S. Er, M. R. Gerhardt,

C. J. Galvin, X. Chen, A. Aspuru-Guzik, R. G. Gordon, M. J. Aziz, *Nature* **2014**, *505*, 195.
[67] K. Lin, R. Gómez-Bombarelli, E. S. Beh, L. Tong, Q. Chen, A. Valle, A. Aspuru-Guzik, M. J. Aziz, R. G. Gordon, *Nat. Energy* **2016**, *1*, 16102.
[68] A. Hollas, X. Wei, V. Murugesan, Z. Nie, B. Li, D. Reed, J. Liu, V. Sprenkle, W. Wang, *Nat. Energy* **2018**, *3*, 508.
[69] a) C. DeBruler, B. Hu, J. Moss, J. Luo, T. L. Liu, *ACS Energy Lett.* **2018**, *3*, 663; b) J. Luo, B. Hu, C. Debruler, T. L. Liu, *Angew. Chem., Int. Ed.* **2018**, *57*, 231.
[70] R. Feng, X. Zhang, V. Murugesan, A. Hollas, Y. Chen, Y. Shao, E. Walter, N. P. N. Wellala, L. Yan, K. M. Rosso, W. Wang, *Science* **2021**, *372*, 836.
[71] T. Liu, X. Wei, Z. Nie, V. Sprenkle, W. Wang, *Adv. Energy Mater.* **2016**, *6*, 1501449.
[72] C. Friebe, A. Lex-Balducci, U. S. Schubert, *ChemSusChem* **2019**, *12*, 4093.
[73] a) V. Singh, S. Kim, J. Kang, H. R. Byon, *Nano Res.* **2019**, *12*, 1988; b) W. Liu, W. Lu, H. Zhang, X. Li, *Chem. - Eur. J.* **2019**, *25*, 1649.
[74] a) T. Janoschka, N. Martin, U. Martin, C. Friebe, S. Morgenstern, H. Hiller, M. D. Hager, U. S. Schubert, *Nature* **2015**, *527*, 78; b) T. Hagemann, M. Strumpf, E. Schröter, C. Stolze, M. Grube, I. Nischang, M. D. Hager, U. S. Schubert, *Chem. Mater.* **2019**, *31*, 7987.
[75] a) T. Sun, J. Xie, W. Guo, D. S. Li, Q. Zhang, *Adv. Energy Mater.* **2020**, *10*, 1904199; b) J. Li, X. Jing, Q. Li, S. Li, X. Gao, X. Feng, B. Wang, *Chem. Soc. Rev.* **2020**, *49*, 3565.
[76] a) B. Sanchez-Lengeling, A. Aspuru-Guzik, *Science* **2018**, *361*, 360; b) S. Er, C. Suh, M. P. Marshak, A. Aspuru-Guzik, *Chem. Sci.* **2015**, *6*, 885.
[77] a) M. Yue, Q. Zheng, F. Xing, H. Zhang, X. Li, X. Ma, *AIChE J.* **2018**, *64*, 782; b) Q. Zheng, F. Xing, X. Li, G. Ning, H. Zhang, *J. Power Sources* **2016**, *324*, 402.
[78] Z. Yuan, H. Zhang, X. Li, *Chem. Commun.* **2018**, *54*, 7570.

Feifei Zhang obtained her Ph.D. degree from Changchun Institute of Applied Chemistry, Chinese Academy of Sciences in 2016. She is currently a research fellow in the Department of Materials Science and Engineering, National University of Singapore. Her recent research interest includes the designing of active materials and catalyst for the aqueous redox flow batteries and the decoupled water splitting.

Qing Wang is currently an Associate Professor at the Department of Materials Science and Engineering, National University of Singapore a professor at National University of Singapore. He obtained his Ph.D. in physics at the Institute of Physics, Chinese Academy of Sciences in 2002. He leads a research group on the fundamental understanding of charge transport/transfer in mesoscopic electrochemical systems and their applications for advanced energy conversion and storage, including the redox targeting-based flow batteries and beyond, with the implementations to a wide variety of battery chemistries and energy materials for advanced energy conversion and storage.